Continental Shelf Research 107 (2015) 115–131

Contents lists available at ScienceDirect

Continental Shelf Research

journal homepage: www.elsevier.com/locate/csr

Research papers

On the salt balance of Tampa Bay

Jun Zhu [a,b], Robert H. Weisberg [a,*], Lianyuan Zheng [a], Hongshuai Qi [b]

[a] College of Marine Science, University of South Florida, St. Petersburg, FL 33701, USA
[b] Third Institute of Oceanography, S.O.A., Xiamen 361005, China

ARTICLE INFO

Article history:
Received 13 May 2014
Received in revised form
29 June 2015
Accepted 4 July 2015
Available online 9 July 2015

Keywords:
Salt balance
Salt flux
Tidal pumping
Modeling
Tampa Bay

ABSTRACT

A three-dimensional, numerical circulation model, with resolution as high as 20 m at important mass conveyances (inlets, channels, bridge causeways, and rivers), is used to diagnose the point by point salt balances for Tampa Bay, FL. While the details of the salt flux divergences and the salt fluxes vary throughout the bay, each is fully three dimensional. On experimental duration (three month) average, the total (horizontal plus vertical) advective salt flux divergence is mainly balanced by the vertical diffusive salt flux divergence, except near the bottom of the deep shipping channel, where horizontal diffusive salt flux divergence is also important. Instantaneously, the local rate of change of salinity is primarily controlled by the advective salt flux divergence, with a secondary contribution by the vertical diffusive salt flux divergence everywhere and the horizontal diffusive salt flux divergence near the channel bottom. To examine the role of tidal pumping, the advective salt fluxes and divergences are further decomposed into the products of the mean salinity and velocity, and the correlation between the salinity and velocity fluctuations. The horizontal and vertical advective salt flux divergences by the mean quantities are equally large and counterbalancing (by continuity), with their sum being a small, but significant residual. The horizontal and vertical advective salt flux divergences due to tidal pumping are relatively small (when compared with the mean quantities) and counterbalancing; but, when summed their residual is comparable in magnitude to that by the mean quantities. So whereas the salt fluxes by tidal pumping are of secondary importance to the salt fluxes by the mean quantities, their total flux divergences are of comparable importance. The salt flux components in all three dimensions (axial, transverse and vertical) themselves vary along the Tampa Bay axis, and these findings may be typical of coastal plain estuaries given their geometrical complexities. Being that the distribution of salt flux bears upon the flux distributions of other scalars (e.g., nutrients, fish larvae, etc.) our findings for salt flux also have broader ecological implications.

1. Introduction

Tampa Bay is a partial to well-mixed estuary located on Florida's west coast. From the Gulf of Mexico at its mouth, the bay extends inland by about 56 km, and it consists of four major segments (Fig. 1): Old Tampa Bay, Hillsborough Bay and Middle and Lower Tampa Bay, each with widths ranging from 8 km to 16 km. The area weighed average depth of Tampa Bay is about 3–4 m, with deeper shipping channels maintained at about 12 m. Fresh water inflows are by four principal rivers, the Hillsborough, Alafia, Manatee, and Little Manatee rivers, with annually averaged discharge rates of about 15 $m^3 s^{-1}$, 13 $m^3 s^{-1}$, 10 $m^3 s^{-1}$, and 6 $m^3 s^{-1}$, respectively, plus numerous other fresh water sources of lesser magnitude (e.g., Lewis and Estevez, 1988). Thus the Tampa Bay circulation is driven by a combination of tides, winds and gravitational convection (e.g., Galperin et al., 1991a, 1991b; Weisberg and Williams, 1991; Weisberg and Zheng, 2006; Meyers et al., 2007), which controls the distribution of salinity and other ecologically important material properties. Given the large variations in water depth and the segmented geometry, the physics associated with the material property balances are not immediately apparent. Here we consider the salt balance as the simplest of these because it is conservative.

Estuarine salt balance studies may be traced back to the James River work of Pritchard (1954). Uncles and Jordan (1979) expanded on this by decomposing the variables of velocity, salinity and water depth into their tidal averages and their variations about the tidal averages. They found that the tidal averaged residual flow, characterized by a seaward flow in the upper layer and a landward flow in the lower layer, dominated the salt transport, with the tidal pumping of salt due to the non-zero correlations between the tidal

* Corresponding author. Fax: +1 727 553 1189.
E-mail address: weisberg@usf.edu (R.H. Weisberg).

http://dx.doi.org/10.1016/j.csr.2015.07.001

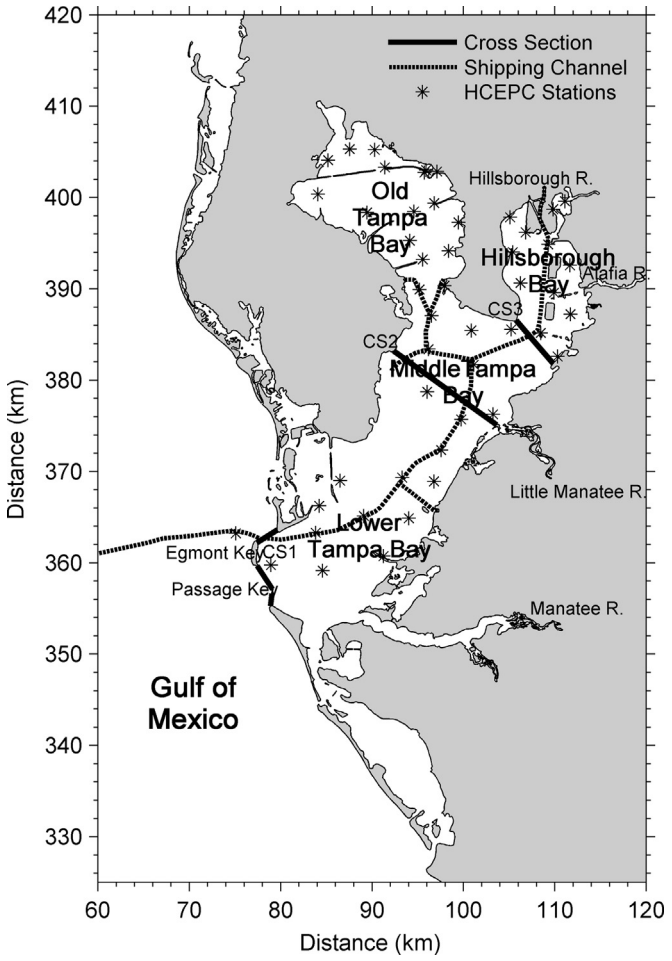

Fig. 1. Tampa Bay and vicinity. The dashed black lines are the shipping channels; the solid black lines (CS1, CS2, and CS3) are the cross sections used in later analyses. The stars are the HCEPC measured stations.

oscillations in velocity and salinity also being of importance. Similar studies were completed by Bowden and Sharaf El Din (1966a, 1966b) and Hansen and Rattray (1965). These studies, by integrating over depth or cross-section, tended to mask the vertical variations in the salt balance mechanisms, including the vertical advection of salt.

A more complicated method, further subdividing each variable into transverse and vertical components, extended the salt transport diagnoses to include the across estuarine axis direction, e.g., Dyer (1974), Dyer et al. (1992), Fischer (1976), Hughes and Rattray (1980), and Rattray and Dworski (1980). Subsequent to these, such decompositions were also applied to analyses of observations, e.g., Becker et al. (2009), Fram et al. (2007), and Lerczak et al. (2006) and model simulations, e.g., Bowen and Geyer (2003), Chen and Sanford (2009), Gong and Shen (2011), MacCready (1999), Ralston et al. (2010), Simpson et al. (2001) and Wu et al. (2010).

These studies in their composite show that estuary salt fluxes are complex, depend on tidal ranges, river inflow magnitudes, and varying bathymetry. For instance, based on velocity profile observations and a simplified frictional balance to extrapolate the flow fields to an entire cross-section, Simpson et al. (2001) found that the salt flux in a tidally energetic, well-mixed estuary is controlled by the seaward salt flux due to the river inflows and the landward salt flux by tidal pumping. In contrast, for the stratified Hudson River estuary, using 43 days of observations, Lerczak et al. (2006) found that the salt flux is mainly controlled by the mean advective and diffusive salt fluxes, except in a region of the lateral constriction where the tidal pumping is also important (Geyer and Nepf, 1996). By combining observations and model simulations for the salt wedge characterized, Merrimack River estuary, Ralston et al. (2010) found the salt flux within the deep channel to be influenced mainly by the tidal asymmetries in halocline elevation and thickness, a form of tidal pumping, whereas the mean advective salt flux was of lesser importance.

In a numerical model study of the Albemarle-Pamlico Sound, a shallow, weakly stratified lagoonal estuary, Jia and Li (2012) decomposed the salt fluxes through selected sections into three terms: sub-tidal (vertically averaged) barotropic, gravitational convection (vertically varying) baroclinic, and tidal pumping. For the inlet connecting the estuary with the inner shelf, the salt flux consisted primarily of tidal pumping (bringing salt in) and the sub-tidal barotropic salt flux (transporting salt out), whereas within the estuary the baroclinic gravitational convection tended to counteract the sub-tidal barotropic salt flux (tending to decrease salt).

All of the above studies diagnosed from one to a few cross sections, or a limited control volume; none of these considered the entire water body or the flux divergences within the water body. Investigations including the vertical salt flux and how this may apportion between the mean flow and the tidal pumping are also limited (Soltaniasl et al., 2013), and the role of turbulent diffusion and how this may apportion between horizontal and vertical contributions remains not well documented.

Studies on the mechanisms that affect Tampa Bay material property balances are particularly sparse. Circulation studies with baroclinicity (and hence estuarine circulation) include Galperin et al. (1991a, 1991b), Weisberg and Williams (1991), Vincent et al. (2000), Weisberg and Zheng (2006), Meyers et al. (2007), Zhang and Wei (2010), and Zhu et al. (2014a). Salt transport is touched upon by Weisberg and Zheng (2006), and flushing either through gravitational convection or the sum of all contributions in aggregate are addressed in Burwell et al. (2000), Weisberg and Zheng (2006), Meyers and Luther (2008) and Zhu et al. (2014b). Unlike transports and flushing based on salinity there are no prior attempts at diagnosing the salt balance for Tampa Bay.

Our paper offers a systematic, point by point, three-dimensional analysis of the Tampa Bay salt fluxes and salt flux divergences comprising the estuary-wide salt balances, including the contributions made by the horizontal and vertical advective salt flux divergences and the horizontal and vertical diffusive salt flux divergences. Our approach is similar to numerical model simulation-based analyses of momentum, e.g., Chen et al. (2001); energy, e.g., Weisberg and Zheng (2003), and temperature, e.g., He and Weisberg (2002, 2003) as applied to other water bodies. Given the non-linearity of the salt balance, we also examine how the advective salt flux divergence apportions into contributions by the experimental duration (three month) averaged mean products and the Reynolds averaged deviations about the mean (primarily due to tidal pumping) and their relative importance to the overall salt balance. Finally, being that Tampa Bay possesses geometries that are typical of the complexities found in many of nature's estuaries, we address the spatial distributions of the salt fluxes per unit area by the mean flow and the tidal pumping at selected cross sections.

The reminder of the paper is organized as follows. Section 2 describes the model and the experimental design. Section 3 defines the analyses based on the salt conservation equation. A decomposition of the advective salt flux divergence into mean and tidal pumping contributions and the three dimensional nature of the salt flux components are given in Sections 4 and 5, respectively. A summary and conclusions follow in Section 6.

2. Model description and experimental design

Our starting point is the Weisberg and Zheng (2006) numerical model simulation of the Tampa Bay circulation. Adapted for Tampa Bay, the adjacent portion of the Gulf of Mexico and peripheral local water bodies (Fig. 2) is the three-dimensional, unstructured grid, Finite Volume Coastal Ocean Model (FVCOM) of Chen et al. (2003). The model uses an unstructured triangular grid in the horizontal and a σ coordinate in the vertical. Turbulence closure vertically is by the Mellor and Yamada (1982) level-2.5 scheme and horizontally by the Smagorinsky (1963) formulation. With resolution increased over its original Tampa Bay application, the revised model grid now has 219,337 triangular elements and 115,369 triangular nodes in the horizontal, and 11 uniformly distributed σ layers in the vertical. The horizontal resolution gradually increases from about 8.5 km along the open boundary to about 20 m within all of the potentially important conveyances of mass, such as the navigation channels, inlets and bridge causeways, the intra-coastal waterway and the adjoining rivers.

As in Weisberg and Zheng (2006), this higher resolution version is initialized on August 24, 2001 and runs through December 1, 2001. To satisfy numerical stability criteria, the external and internal mode time steps are 0.3 s and 1.2 s, respectively. External forcing consists of eight principal tidal harmonic constants along the open boundary extracted from the Oregon State University tidal inversion software (Egbert and Erofeeva, 2002), plus daily river discharge rates from both USGS river gauges and the Tampa Bay PORTS program with the sum of the freshwater discharge rates varying between around 250 m^3/s at the beginning and decreasing to around 25 m^3/s at the end of the experiment. With temperature variation effects on density being insignificant relative to salinity, temperature is held constant at 20 °C. Salinity is initialized by interpolating from a lower resolution FVCOM model simulation for the west Florida shelf (WFS) that begins on January 1, 2001 and includes Tampa Bay with a resolution of about 150 m (e.g., Zheng and Weisberg, 2012).

With the salinity initialization already baroclinically adjusted to the external forcing over the previous eight months (i.e., the initialization includes a balanced horizontal salinity gradient), only a relatively short frictional spin up time is required for the present simulation. Thus we discard the first week of the model run and use the remaining 91 days from September 1 to December 1, 2001 for analyses. A more detailed model description is provided by Zhu et al. (2014a), where fidelity is found between the model simulation and observations for the circulation contributions made by tides, winds and rivers, and this fidelity is slightly better (by virtue of increased resolution) than that found in Weisberg and Zheng (2006). Given the established model fidelity, Zhu et al. (2014b) made additional applications to the flushing of Tampa Bay as a whole and for selected sub-regions. Our further application here is to the salt balance. The only difference between the Zhu et al. (2014a, 2014b) applications and the present work is that for simplicity we now omit wind forcing, enabling us to equate the Reynolds fluxes to fluxes by tidal pumping without the added variances that may have been associated with synoptic scale wind variations.

Unlike the time series observations for velocity and sea level, the observations for salinity are sparse and non-synoptic. They consist of monthly samples at near surface and near bottom locations collected by the Hillsborough County Environmental Protection Commission (HCEPC). By the nature of the sampling (not at precise locations or depths and aliased by tides), these data are most amenable to mapping when averaged over many samples. Thus for our purposes, we objectively mapped the HCEPC observations onto a uniform grid and then performed a climatological September through November average over the years 1998 through 2004, thereby bracketing the 2001 period modeled herein. Fig. 3a compares our modeled September through November 2001 surface salinity average with the HCEPC diagnosed climatological (1998–2004) September through November surface salinity, showing that the modeled and observed patterns of bay-wide salinity are similar. Fig. 3b further compares the modeled

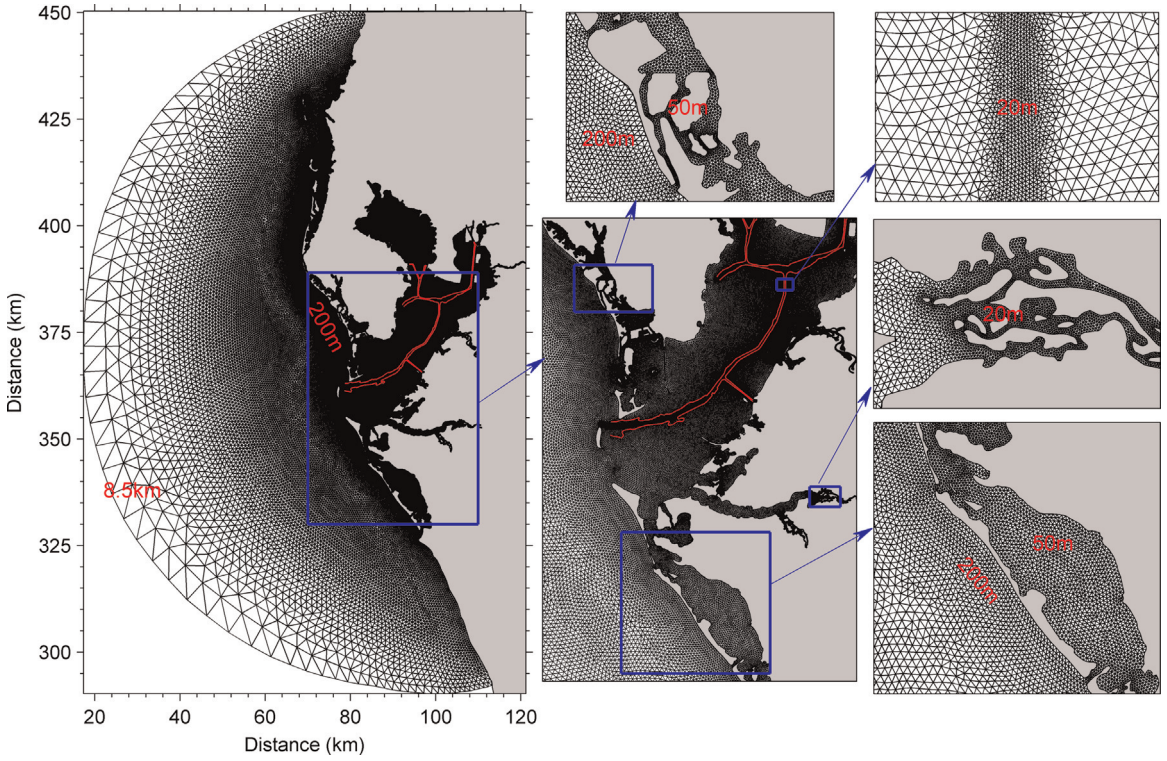

Fig. 2. The entire unstructured model grid, plus zoomed views of selected sub-regions for the purpose of highlighting the resolution that is achieved.

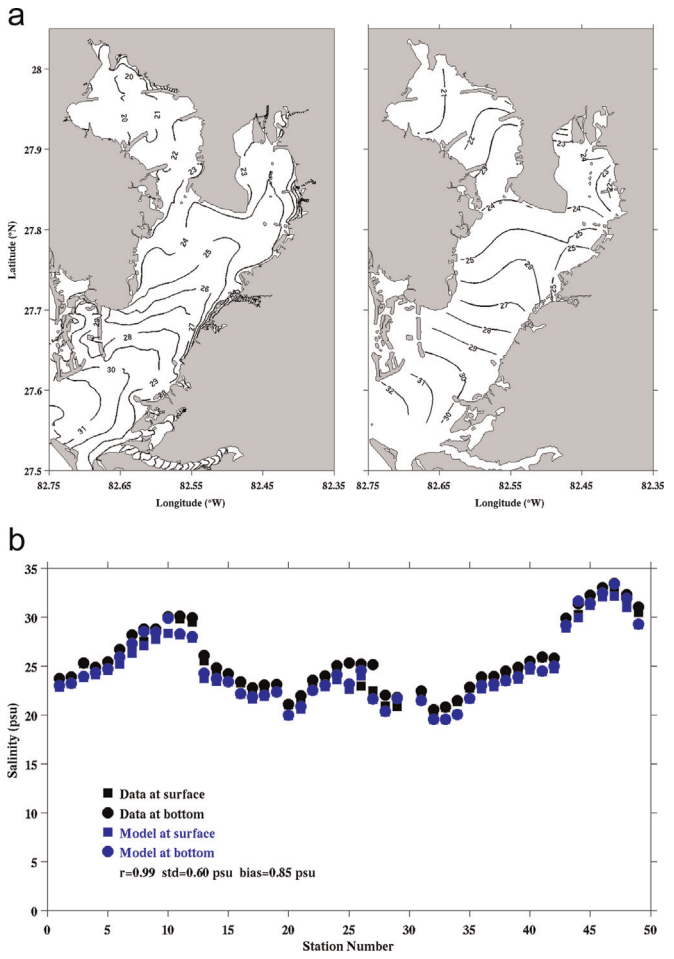

Fig. 3. (a) A comparison between Tampa Bay surface salinities, as modeled (left hand panel) and observed (right hand panel). The modeled values are averaged over the experimental duration, September through November, 2001. The observed values are climatologically averaged for September through November over 1998 through 2004. As explained in the text, a climatological average is necessary because the observations (made by the Hillsborough County Environmental Protection Commission) are sparsely sampled and aliased by tides and winds. For instance, the sparseness in sampling is why the observations barely discriminate the shipping channel. Nonetheless the overall patterns are similar throughout the bay and the magnitudes are generally within a salinity unit of one another. (b) A comparison between modeled and observed surface and bottom salinity at HCEPC observational stations. The modeled values (blue) are averaged over the experimental duration, September through November, 2001. The observed values (black) are climatologically averaged for September through November over 1998 through 2004. The squares are for surface and circles are for bottom salinities. r, std, and bias are the correlation coefficient between modeled and observed salinity, standard deviation and bias of the modeled and observed salinity differences, respectively. (For interpretation of the references to color in this figure legend, the reader is referred to the web version of this article.)

(blue) and observed (black) surface (squares) and bottom (circles) salinities at each of the 49 HCEPC stations that span the bay (Fig. 1). The observed Tampa Bay salinities range from about 19–34 psu. While the observed surface to bottom salinity difference is larger in the deeper than in the shallower regions, the mean difference between the observed surface and bottom salinity is 0.6 psu, and the overall mean vertical salinity gradient is less than 0.2 psu/m. Given a correlation coefficient of 0.99, a standard deviation of 0.6 psu and a bias of 0.85 psu between the modeled and observed salinities, Fig. 3a and b demonstrates that the model is adequately accounting for the Tampa Bay salinity distributions in magnitude and in both the horizontal and vertical salinity gradient components. These salinity findings, coupled with the detailed velocity and sea level time series comparisons (Zhu et al., 2014b; Weisberg and Zheng, 2006) justify our use of the model simulation for diagnosing the salt balance (through the salt fluxes and the salt flux divergences).

The salt conservation Eq. (1), written with respect to the σ coordinate, provides the basis for our term-by-term salt balance analyses:

$$\frac{\partial SD}{\partial t}+\frac{\partial SuD}{\partial x}+\frac{\partial SvD}{\partial y}+\frac{\partial \omega S}{\partial \sigma} = \frac{\partial}{\partial x}\left(K_h D\frac{\partial S}{\partial x}\right)+\frac{\partial}{\partial y}\left(K_h D\frac{\partial S}{\partial y}\right)+\frac{1}{D}\frac{\partial}{\partial \sigma}\left(K_v\frac{\partial S}{\partial \sigma}\right) \quad (1)$$

where x and y are the east and north coordinates and σ is the vertical coordinate, varying from -1 at the bottom to 0 at the surface; u, v and ω are the x, y, and σ velocity components; t is the time; S is the salinity; K_h and K_v are the horizontal and vertical scalar diffusion coefficients, respectively, and D is the total water depth. We note that the FVCOM method of solution for Eq. (1) is to integrate over individual control volumes using Green's Theorem to calculate the horizontal advective flux divergence. The rate of change of salinity for each of salt terms is defined and calculated as follows:

(I) $\frac{1}{\langle D\rangle}\frac{\partial SD}{\partial t}$ is the local rate of salinity change, where the angled bracket indicates a time mean;
(II) $-\frac{1}{\langle D\rangle}\frac{\partial SuD}{\partial x}-\frac{1}{\langle D\rangle}\frac{\partial SvD}{\partial y}$ is the horizontal advective salt flux divergence;
(III) $-\frac{1}{\langle D\rangle}\frac{\partial S\omega}{\partial \sigma}$ is the vertical advective salt flux divergence;
(IV) $\frac{1}{\langle D\rangle}\frac{\partial}{\partial x}\left(K_h D\frac{\partial S}{\partial x}\right)+\frac{1}{\langle D\rangle}\frac{\partial}{\partial y}\left(K_h D\frac{\partial S}{\partial y}\right)$ is the horizontal diffusive salt flux divergence;
(V) $\frac{1}{\langle D\rangle}\frac{1}{D}\frac{\partial}{\partial \sigma}\left(K_v\frac{\partial S}{\partial \sigma}\right)$ is the vertical diffusive salt flux divergence.

After term-by-term analysis of the salt balance equation, we further decompose the advective salt flux divergence components into time averaged (over the experimental duration of three months) and oscillatory parts. Thus we separate the instantaneous variables, u, v, ω, S, and D into two parts according to:

$$\phi = \langle\phi\rangle + \phi' \quad (2)$$

where ϕ refers to u, v, ω, S, and D, the angled brackets refer to the time averaged part, and the prime indicates the oscillatory part. With this Reynolds decomposition, the record length mean advective salt flux components are given by:

$$\langle SuD\rangle = \langle uD\rangle\langle S\rangle + \langle S'u'\rangle\langle D\rangle + \langle S'D'\rangle\langle u\rangle + \langle S'u'D'\rangle \quad (3)$$

$$\langle SvD\rangle = \langle vD\rangle\langle S\rangle + \langle S'v'\rangle\langle D\rangle + \langle S'D'\rangle\langle v\rangle + \langle S'v'D'\rangle \quad (4)$$

$$\langle S\omega\rangle = \langle S\rangle\langle\omega\rangle + \langle S'\omega'\rangle \quad (5)$$

Whereas $\langle uD\rangle\langle S\rangle$ may be further decomposed into salt fluxes due to the Eulerian residual flow and the Stokes drift (Uncles and Jordan, 1979; MacCready, 1999), being that the two terms are inherently associated with the advection of mean salinity by the water volume flux, we keep them together.

Substituting (3) and (4) into (II) yields

$$\underbrace{-\frac{1}{\langle D\rangle}\frac{\partial\langle SuD\rangle}{\partial x}-\frac{1}{\langle D\rangle}\frac{\partial\langle SvD\rangle}{\partial y}}_{\text{(II)}} = \underbrace{-\frac{\partial[\langle uD\rangle\langle S\rangle]}{\langle D\rangle\partial x}-\frac{\partial[\langle vD\rangle\langle S\rangle]}{\langle D\rangle\partial y}}_{\text{(VI)}} \underbrace{-\frac{\partial\left[\langle S'u'\rangle\langle D\rangle\right]}{\langle D\rangle\partial x}-\frac{\partial\left[\langle S'v'\rangle\langle D\rangle\right]}{\langle D\rangle\partial y}}_{\text{(VII)}} \underbrace{-\frac{\partial\left[\langle S'D'\rangle\langle u\rangle\right]}{\langle D\rangle\partial x}-\frac{\partial\left[\langle S'D'\rangle v\right]}{\langle D\rangle\partial y}}_{\text{(VIII)}} \underbrace{-\frac{\partial\langle S'u'D'\rangle}{\langle D\rangle\partial x}-\frac{\partial S'v'D'}{\langle D\rangle\partial y}}_{\text{(IX)}} \quad (6)$$

The first term, VI, on the right hand side of Eq. (6) is the horizontal advective salt flux divergence due to horizontal mean flow,

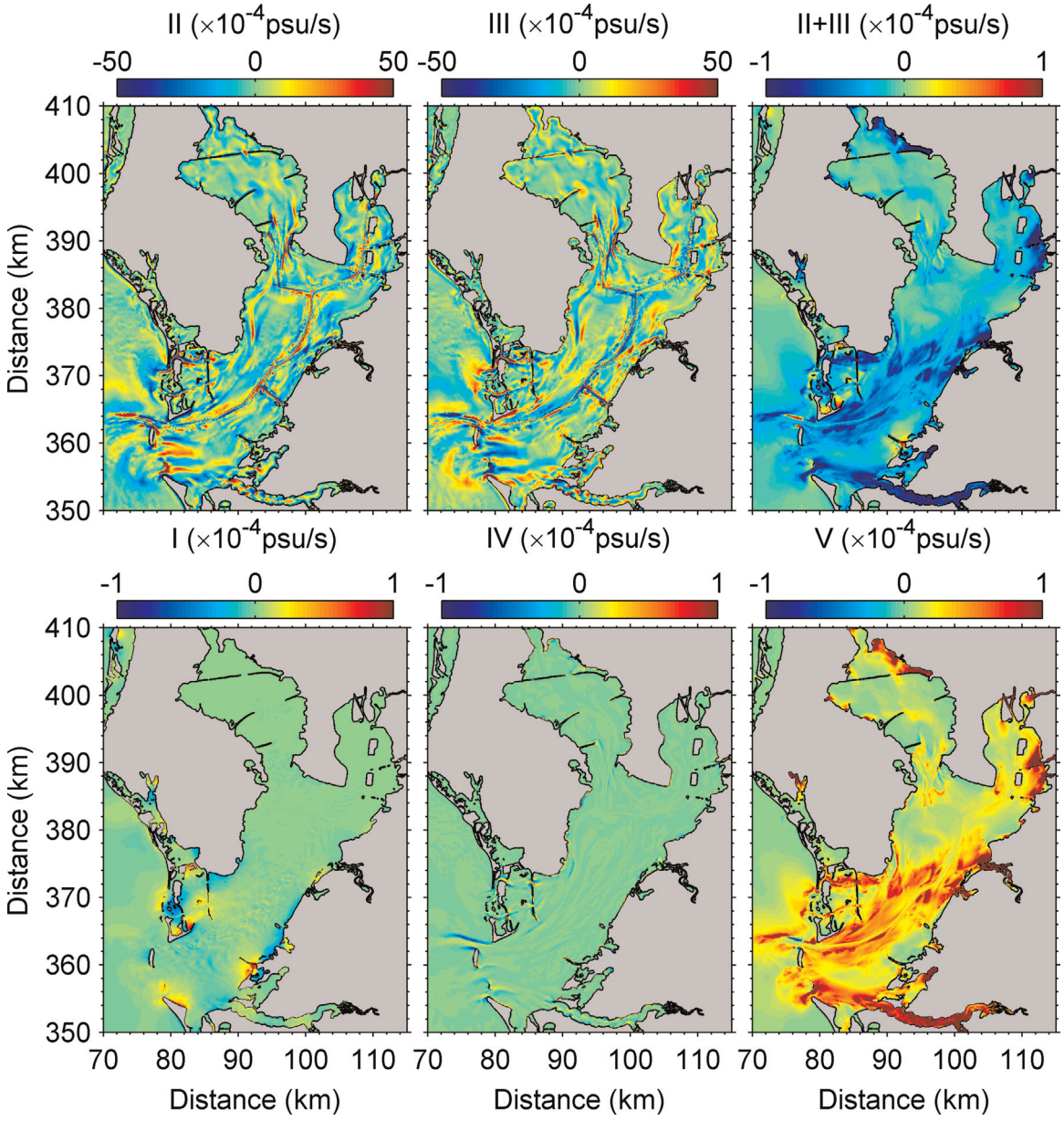

Fig. 4. The structures of the salt balance terms evaluated at surface. Clockwise from the upper left are the horizontal (II) and vertical (III) advective salt flux divergences and their sum (II+III), followed below by the vertical (V) and horizontal (IV) diffusive salt flux divergences and lastly the local rate of change of salt (I). Note the magnitude differences as given by the colorbar scales for each panel. (For interpretation of the references to color in this figure legend, the reader is referred to the web version of this article.)

and the second term, VII, represents the horizontal advective salt flux divergence due to the horizontal Reynolds' fluxes (or the non-zero correlation between the oscillations in salinity and velocity) that we will refer to as tidal pumping [previously called the tidal oscillatory component by Bowen and Geyer (2003)]. The last two terms, VIII and IX, in the Eq. (6) represent the advective salt flux divergence parts due to the non-zero correlation between the oscillations in water depth and salinity and the triple correlation between the tidal oscillations in velocity, salinity and water depth, respectively, both of which are found to be very small (not shown) and neglected here, consistent with the findings of Hughes and Rattray (1980).

Combining (5) and (III) yields

$$\underbrace{-\frac{1}{\langle D\rangle}\frac{\partial\langle S\omega\rangle}{\partial\sigma}}_{\text{(III)}} = \underbrace{-\frac{\partial[\langle S\rangle\langle\omega\rangle]}{\langle D\rangle\partial\sigma}}_{\text{(X)}} \underbrace{-\frac{\partial\langle S'\omega'\rangle}{\langle D\rangle\partial\sigma}}_{\text{(XI)}} \quad (7)$$

The first term, X, on the right hand side of Eq. (7) represents the advective salt flux divergence due to the vertical mean flow, and the second term, XI, represents the advective salt flux divergence by vertical tidal pumping.

Calculations of the overall mean terms in Eq. (1) are performed on line, whereas the use of mean variables and deviations about the means require offline processing. Thus beginning on September 1, 2001 each of the modeled variables at each of the model points are saved hourly, and it is from these hourly values that the Reynolds' decomposition is performed (mean fluxes and Reynolds fluxes). Derivative terms for these Reynolds' decompositions are then calculated following the FVCOM methods. Hence a combination of online and offline methods are used to arrive at terms (I) through (XIV). Section 3 provides the overall means (by direct on-line calculation) and Section 4 adds the Reynolds decomposition (by off-line calculation using saved hourly values).

3. Overall salt balance diagnosis

The decomposition of the salt balance Eq. (1) allows us to diagnose the apportionment of the balance into the various terms defined above and to assess how these vary spatially throughout Tampa Bay. We note that the salt flux and the salt flux divergence terms are all calculated along σ layers. Thus for the horizontal terms to indeed be horizontal, an adjustment must be made to compensate for the difference between the σ and Cartesian (z) coordinate orientations (e.g., Kantha and Clayson, 2000, pp. 588–589). By including this adjustment in the vertical term, continuity and the robustness of the fully three dimensional salt flux divergence are maintained. We mention this for completeness, while noting that such adjustments are generally minor except where flows tend to cross regions of large topographic gradient.

3.1. Baywide structures at the surface and bottom

We begin with a determination of the experimental duration (three month) average surface salinity balance, as shown in Fig. 4. Clockwise from the upper left, the panels depict the horizontal (II) and vertical (III) advective salt flux divergences and their sum (II+III, total advective salt flux divergences), followed below by the vertical (V) and horizontal (IV) diffusive salt flux divergences and lastly the local rate of change of salt (I). The magnitudes of the terms are color coded with different scales. Note first that the horizontal advective flux divergence (II) and the vertical advective flux divergence (III) are each of opposite sign and approximately an order of magnitude larger than all of the other terms. As Whitney and Allen (2008) pointed out, the opposing signs and large magnitudes of terms (II) and (III) derive, in part, from the continuity equation. Upon summation this continuity contribution is removed leaving the total advection of salt. The sum of terms (II) and (III) shows a fairly uniform spatial distribution, evincing a

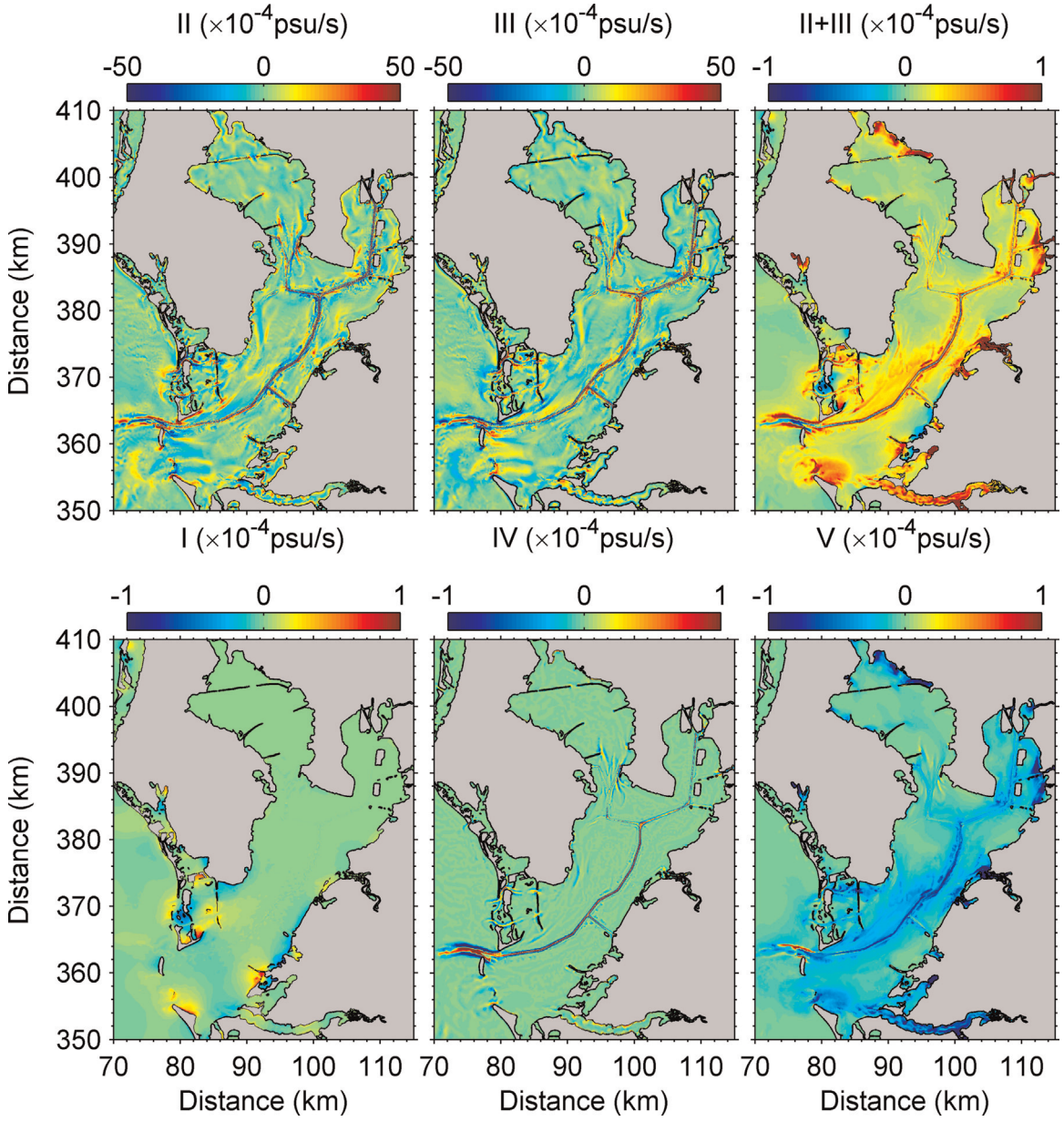

Fig. 5. Same as Fig. 4, except for the near bottom layer. (For interpretation of the references to color in this figure legend, the reader is referred to the web version of this article.)

decreasing salinity tendency at the surface that is balanced in large measure by term (V). Term (IV) is small at the surface and the sum of all terms (II+III+IV+V) equals a similarly small local rate of change term (I). Thus salt advection at the surface tends to decrease salinity, and this tendency is offset by turbulent diffusion in the vertical that mixes saltier water at depth into the fresher surface waters, and this finding is consistent with the classical view on the salinity balance for a partially mixed estuary (e.g., Pritchard, 1954). The finding of relatively small horizontal diffusive salt flux divergence at the surface is consistent with the general (anecdotal) observation in most estuaries of surface slicks and fronts that extend over large distances (recall, for instance, tidal slicks consisting of organic matter that are seen to emanate from bridge pilings). That the independently calculated experimental duration local rate of change term I essentially equals the sum of the other terms (with a relative error of less than 10^{-2} times I) attests to the veracity of the calculation.

The salt balances near the bottom (Fig. 5) are similar to those at the surface (Fig. 4) with two major exceptions. The primary balance is again between the total advective salt flux divergence (a small residual between nearly compensating horizontal and vertical contributions) and vertical diffusion, but now with the signs reversed, i.e., opposite from the surface, advection tends to increase near bottom salinity, whereas vertical diffusion tends to decrease it. Secondly, horizontal diffusion tends to be important within the main shipping channels, where the across channel derivatives may be large due to the relatively steep channel side walls. Despite these two differences, it is noted that the experimental duration averaged local rate of salinity change is again very small, as expected.

The relative importance of the total advective salt flux divergence (II+III) and the vertical (V) and horizontal (IV) diffusive salt flux divergences to the overall salt balance may be quantified by a dimensionless ratio, r_Y, defined as:

$$r_Y = \frac{\sqrt{\overline{Y}^2}}{\sqrt{\overline{(\mathrm{II}+\mathrm{III})}^2} + \sqrt{\overline{\mathrm{IV}}^2} + \sqrt{\overline{\mathrm{V}}^2}} \tag{8}$$

where Y refers to II+III, IV or V; and the overbar denotes an area weighted average for each of these constituents. Table 1 provides the r_Y results at the surface and near bottom, showing the contrast in importance of horizontal diffusion between these two planar sections.

3.2. Cross-sectional distributions

Complementing the planar views of the salt balances at the surface and near the bottom, we now consider the balances for two cross sections, one at the Tampa Bay Mouth (CS1) and the other at a Middle Tampa Bay (CS2) location provided in Figs. 6 and 7, respectively, where the clockwise ordering of terms is the same as in Figs. 4 and 5. The salt balances at CS1 and CS2 differ greatly in complexity. As in the planar views the horizontal (II) and vertical (III) advective salt flux divergences tend to be large and counterbalancing. The increased complexity in their spatial structure derives from the variations in bottom topography. This coupled with the narrow channels and swifter currents at the bay mouth (particularly within Egmont Channel) and the associated secondary circulations (e.g., Nunes and Simpson, 1985), increases the salt balance complexity there. Moreover, and in parallel with the planar view near bottom balances (Fig. 5), the horizontal diffusive salt flux divergence (IV) plays a role along with the vertical diffusive salt flux divergence (V) in the salt balance. When spatially averaged over cross section CS1 these three terms (II+III, IV and V) contribute 0.40, 0.48 and 0.12, respectively, to the local salt balance (Table 1).

Table 1
Ratios of the contributions made to the mean local rate of change of salt (I) by the total advective salt flux divergence (II+III), the horizontal diffusive salt flux divergence (IV) and vertical diffusive salt flux divergence (V).

	II+III	IV	V
Surface (Fig. 4)	0.47	0.06	0.47
Bottom (Fig. 5)	0.37	0.37	0.26
Cross section CS1 (Fig. 6)	0.40	0.48	0.12
Cross section CS2 (Fig. 7)	0.42	0.24	0.34

The salt balance for the Middle Tampa Bay cross section, CS2, with less radical topography, is simpler (Fig. 7) than that at CS1. Whereas secondary circulation effects are evident in the two shipping channels (each of much lesser depth than at the bay mouth's Egmont Channel) and in the shoals in between, the overall magnitudes of the advective salt flux divergences (II and III) are smaller than at CS1 and their addition (II+III) evinces a much simpler pattern. Seen at CS2 is the tendency by advection to decrease salinity over the upper portion of the water column and to increase salinity over the lower portion, with these tendencies perturbed only in the deepest portion of the main shipping channel. Balancing these total advective salt flux divergence tendencies (II+III) are the vertical diffusive salt flux divergence tendencies (V), with opposite signs over the upper and lower portions of the water column. An exception noted is at the deepest portion of the main shipping channel, where, as in Fig. 5, the horizontal diffusive salt flux divergence tendency (IV) also comes into play.

The horizontal diffusive salt flux divergence being small at the surface and large near the bottom of the deep shipping channels is physically plausible for the reason already given (large gradients and curvatures). We may rule out numerical diffusion for two reasons, the first being the small values at the surface relative to the bottom and the second being a demonstration with our Tampa Bay FVCOM applied to passive tracer dispersion under differing forcing functions (see an example in Weisberg (2011)).

Thus far the salt balance diagnoses (Figs. 4–7) have concerned the experimental duration (three month) mean values. It is also instructive to see how these may vary on the tidal time scale. Fig. 8a shows the evolution of the terms comprising the salt budgets over nearly one neap–spring tide cycle at CS1 sampled at the surface (left hand panels) and near the bottom (right hand panels). The ordinate is distance across the bay mouth from the northern shore of Egmont Channel on the top (0 km) of each panel to the southern shore of the Tampa Bay mouth (~8 km) on the bottom of each panel. Either at the surface or near the bottom, the tendency is for the local rate of change of salinity (I) to be attributed to the total advective rate of change of salinity, with the vertical diffusive rate of change (V) comprising their difference at the surface, whereas both the vertical diffusive rate of change (V) and the horizontal diffusive rate of change (IV) together comprise their difference near the bottom. The modulation of these balances by the neap–spring tide range is not large.

Also of interest is the finding that the instantaneous rates of change of salinity over the southern portion of the bay mouth (to either side of Passage Key) show larger values than that in Egmont Channel, primarily because the salinity gradient is larger at Passage Key due to fresh water input locally by the Manatee River. Despite the instantaneous rates of salinity change being larger near Passage Key than in Egmont Channel, the latter is the primary conveyance for Tampa Bay salt transport on average, as will be shown later. Finally, the instantaneous variations at the Middle Tampa Bay cross section, CS2, are similar to those at CS1, i.e., the local rate of salinity change is due primarily to the total advective rate of change, with secondary contributions from vertical diffusion at the surface and with a combination of vertical and

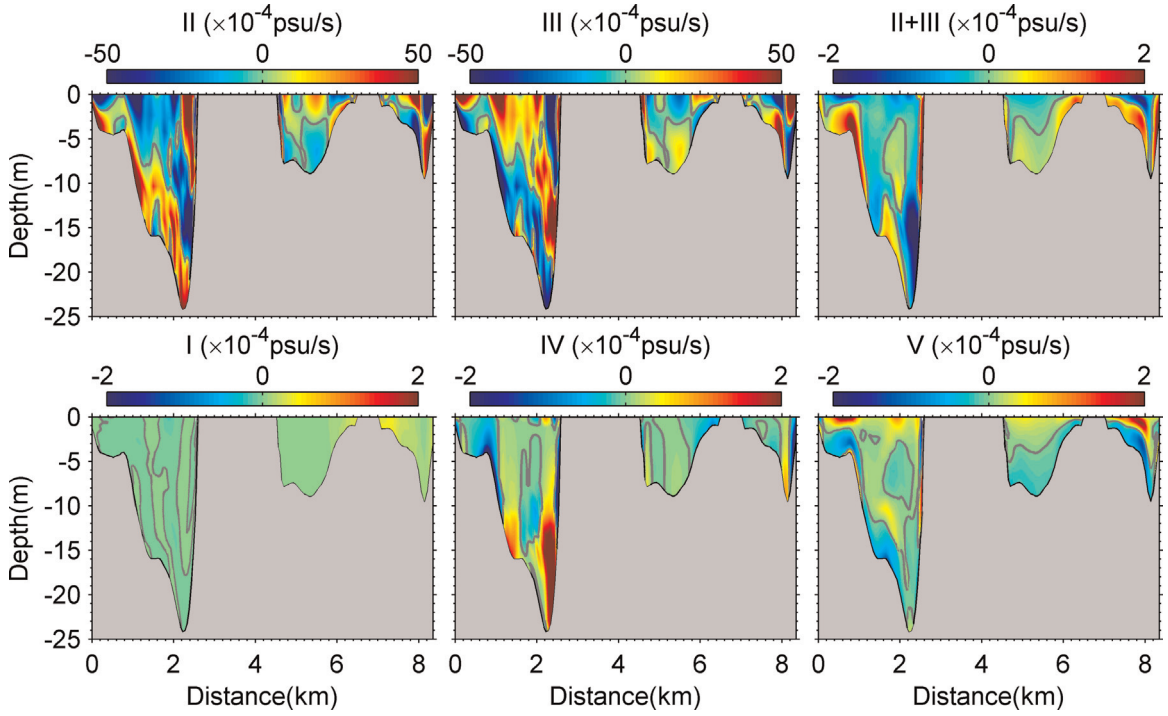

Fig. 6. The structures of the salt balance terms evaluated at the Tampa Bay Mouth cross section CS1. Clockwise from the upper left are the horizontal (II) and vertical (III) advective salt flux divergences and their sum (II+III), followed below by the vertical (V) and horizontal (IV) diffusive salt flux divergences and lastly the local rate of change of salt (I). Note the magnitude differences as given by the colorbar scales for each panel. (For interpretation of the references to color in this figure legend, the reader is referred to the web version of this article.)

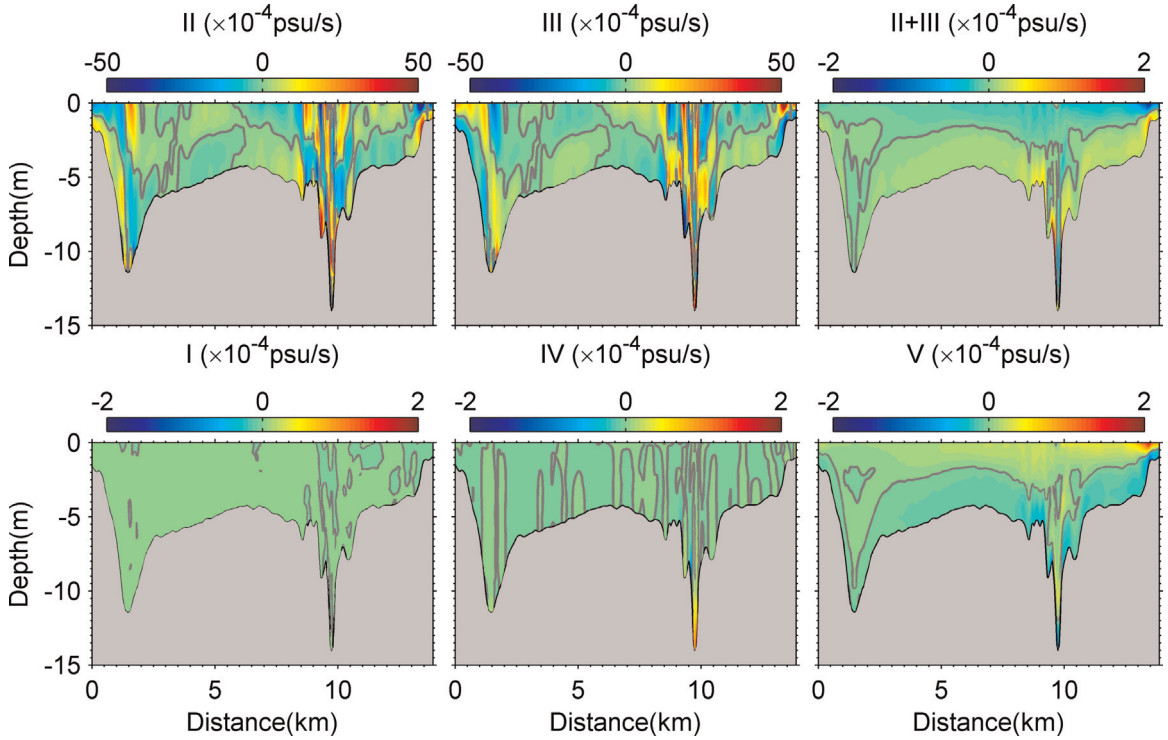

Fig. 7. Same as Fig. 6, except for the Middle Tampa Bay cross section CS2. (For interpretation of the references to color in this figure legend, the reader is referred to the web version of this article.)

horizontal diffusion near the bottom.

Whereas the instantaneous balances are primarily due to the advective and local rates of change, upon averaging to filter out the tides, the balances change to being primarily due to the advective and diffusive rates of change. This is seen in Fig. 8b, which is the same as Fig. 8a, but low-pass filtered (using a 36 h cut-off) to average out the tides. As with the instantaneous balances, the neap–spring tide modulation of these low pass filtered balances is not large. Considering that the record length average is over about six such neap–spring cycles, any biasing of the record length averaged results by neap–spring tide modulation is negligible. For instance, when checking products such as $< us >$ between low-

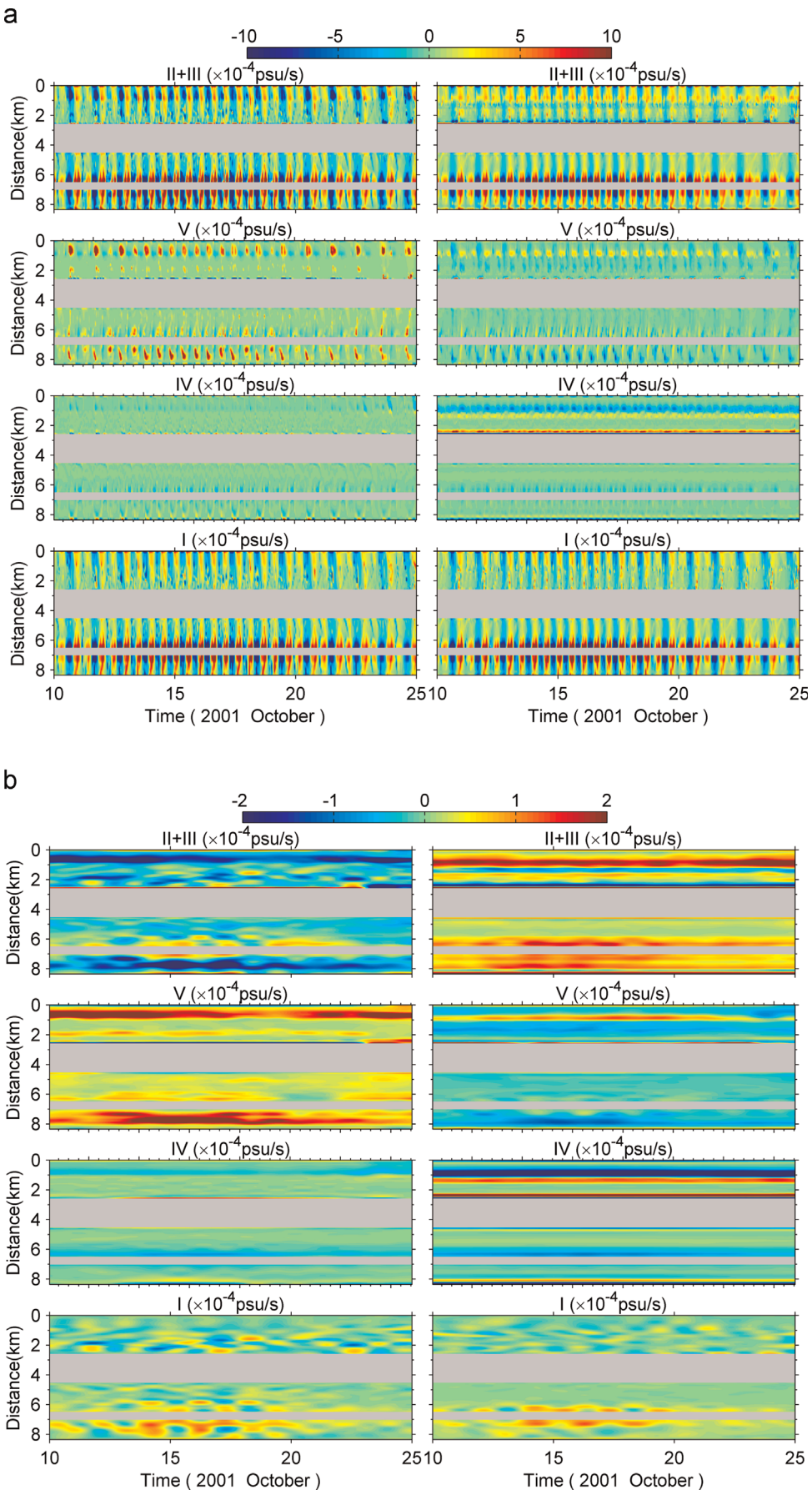

Fig. 8. A 15 day temporal evolution of the salt balance terms through nearly one spring–neap tide cycle evaluated at the Tampa Bay Mouth cross section CS1. The left and right hand panels are for the surface and the near bottom, respectively. As in Fig. 6, the enumerated terms are the local rate of change of salt (I), the horizontal (II) and vertical (III) advective salt flux divergences and their sum (II+III), and the vertical (V) and horizontal (IV) diffusive salt flux divergences.

pass filtered and non-filtered versions we found differences of only about 1%.

4. Reynolds' decomposition of the salt advection

Section 3 described the salt balances, both on average and instantaneous. The junction between these two viewpoints is the non-linear interaction that may occur between the velocity and salinity variations, especially on the tidal time scale for which the velocity and salinity variations are large. This section describes how the advective contributions to the salt balance apportion between mean quantities and the deviations about the means, primarily due to tides in this simulation. The Reynolds' decompositions of Section 2 apply and, in particular, terms (VI) and (X) for the horizontal and vertical advective salt flux divergences associated with the mean quantities, respectively, and terms (VII) and (XI) for the horizontal and vertical advective salt flux divergences associated with the tidal variations about the mean quantities, respectively. As in Nepf and Geyer (1996), these latter fluctuating quantities are referred to as tidal pumping. Had we included wind forcing then we may have opted to separate the tidal interactions as in Lerczak et al. (2006).

4.1. Baywide structures at the surface and near bottom

On experimental duration (three month) average, the advective salt flux divergences due to the horizontal mean flow (VI) and the horizontal tidal pumping (VII) in Eq. (6), and the vertical mean flow (X) and the vertical tidal pumping (XI) in Eq. (7) are given for the surface and near bottom in Fig. 9 and Fig. 10, respectively. In each of these figures the top panels show the mean flow terms (VI) and (X) and their sum (VI+X), and the bottom panels show the tidal pumping terms (VII) and (XI) and their sum (VII+XI). We

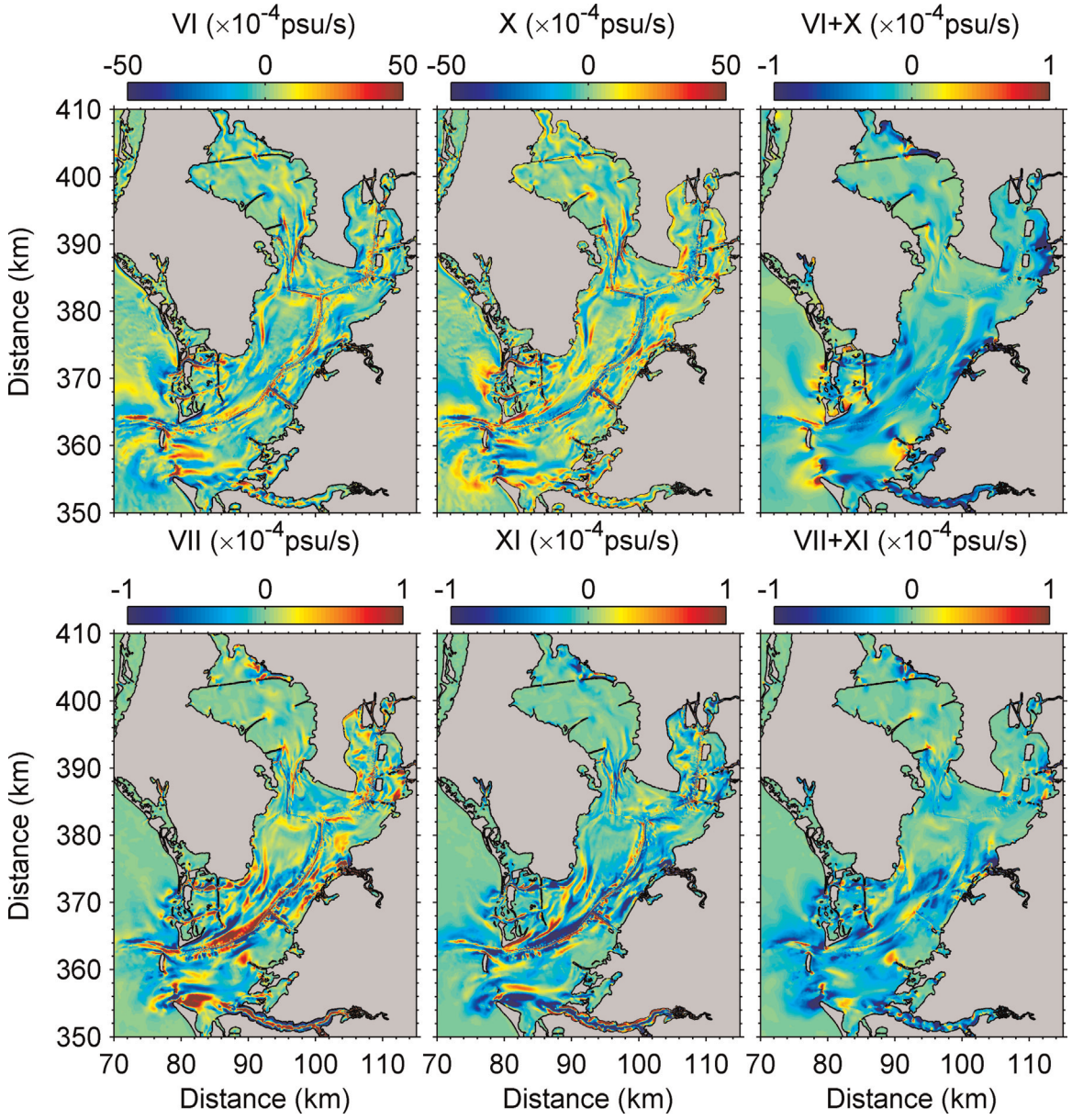

Fig. 9. The structures of the advective salt flux divergence terms after decomposition into mean and tidal pumping contributions evaluated at the surface. The top panels show the horizontal and vertical mean flow terms (VI) and (X), respectively, and their sum (VI+X), and the bottom panels show the horizontal and vertical tidal pumping terms (VII) and (XI), respectively and their sum (VII+XI). Note that the mean flow terms (VI) and (X) are an order of magnitude larger than the tidal pumping terms (VII) and (XI), as indicated by the different colorbar scales. (For interpretation of the references to color in this figure legend, the reader is referred to the web version of this article.)

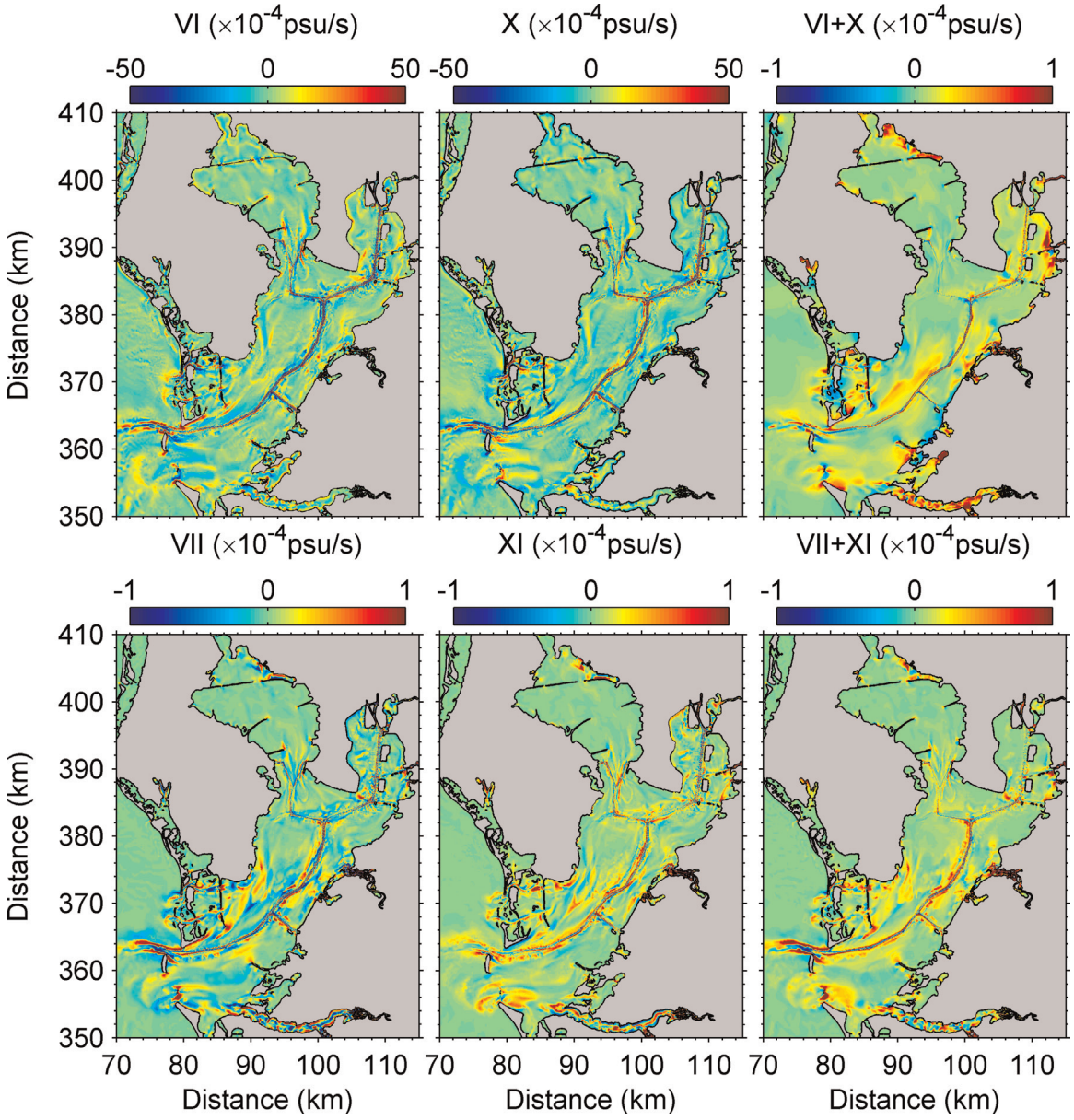

Fig. 10. Same as Fig. 9, except for evaluation in the near bottom layer. (For interpretation of the references to color in this figure legend, the reader is referred to the web version of this article.)

note that the mean flow terms (VI) and (X) are an order of magnitude larger than the tidal pumping terms (VII) and (XI). We further note that (as before in Section 3) the horizontal and the vertical terms, whether they are means or tidal pumping, tend to counterbalance one another. Upon addition the patterns are simplified and the order of magnitude for the sum (VI+X) is greatly reduced to be equal and of similar sign to (VII+XI). Upon adding these together (VI+X+VII+XI) to get the total advective salt flux divergence by the means, plus the tidal pumping, we duplicate (not shown) the upper right hand panels of Figs. 4 and 5 for the surface and near bottom, respectively, i.e., the terms (II+III) before they were subjected to the mean and tidal pumping decomposition. This provides a consistency check on our analysis methods [i.e., we arrive at similar results by online (Section 3) and offline (Section 4) methods].

Similar to calculating the relative contributions of II+III, IV, and V in the salt balance, we may now further evaluate the contribution ratios of the advection salt flux divergences due to the mean flow (VI+X) and the tidal pumping (VII+XI) according to

$$r_Y = \frac{\sqrt{\overline{Y}^2}}{\sqrt{\overline{(\mathrm{VI}+\mathrm{X})}^2} + \sqrt{\overline{(\mathrm{VII}+\mathrm{XI})}^2}} \tag{9}$$

where Y refers to either VI+X or VII+XI, and the overbar again refers to an area weighted average. The contribution ratios of VI+X, and VII+XI are 0.59 and 0.41 for the surface, respectively, and 0.53 and 0.47 for the near bottom, respectively (Table 2). Thus not only are the advective salt flux divergences in the horizontal and vertical directions nearly equal and opposite, their apportionment into total (three-dimensional) mean and total tidal pumping contributions are nearly equal. For Tampa Bay the advective salt flux divergence contribution to the salt balance is fully three dimensional and the correlation between the tidally varying velocity and salinity (tidal pumping) is as important in the mean salinity balance as the mean flow is itself. This is despite the finding that the individual (horizontal and vertical) tidal pumping terms themselves are an order of magnitude smaller than their mean flow counterparts (by reason of the continuity equation as

Table 2
Ratios of the contributions made to the total advective salt flux divergence (II+III) by the advective salt flux divergences due to mean flow (VI+X) and the tidal pumping (VII+XI).

	VI+X	VII+XI
Surface (Fig. 9)	0.59	0.41
Bottom (Fig. 10)	0.53	0.47
Cross section CS1 (Fig. 11)	0.48	0.52
Cross section CS2 (Fig. 12)	0.51	0.49

explained earlier).

4.2. Cross-sectional distributions

An analysis similar to that of Section 4.1 for the surface and near bottom planar distributions is performed for the Tampa Bay Mouth (CS1) and Middle Tampa Bay (CS2) cross sections, as given in Figs. 11 and 12, respectively. As with the planar distributions, the cross section distributions also show counterbalancing horizontal and vertical salt flux divergences, which, when summed, take on a simpler appearance than before summation. Also the contributions by the total mean quantities and the total tidal pumping are of similar magnitude. Summing the mean quantities (VI+X) and the tidal pumping (VII+XI), i.e., the upper and lower right hand panels in Figs. 11 and 12, respectively, results in the upper right hand panels of Figs. 6 and 7 for the section CS1 and CS2, respectively.

New in the cross sectional views, and not as readily apparent from the planar views, is the cellular nature of the advective salt flux divergences. For instance, the advective salt flux divergences associated with either the horizontal (VII) or the vertical (XI) tidal pumping are much larger than their sum (VII+XI) and with a pattern of alternating signs throughout the cross section, perhaps more easily seen in the simpler of the two cross sections CS2. These alternating cells are likely associated with the secondary circulations set up by bottom topography and stratification (e.g., Nunes and Simpson, 1985; Chant, 2002; Lerczak and Geyer, 2004). As an example, MacCready and Geyer (2010) describe counter-rotating circulations besides a deep channel due to a lateral density gradient yielding convergence at the surface and divergence near the bottom. These secondary circulation structures are also reported in the previous Tampa Bay work of Weisberg and Zheng (2006), where the mean salinity field results in a surface dynamic height distribution, with concavity across the main channel causing convergence there.

In terms of the ratios previously defined, the contributions of the advective salt flux divergence due to the total mean flow, VI+X, and the total tidal pumping, VII+XI, are 0.48 and 0.52, respectively, when area averaged over CS1, and 0.51 and 0.49 when area averaged over CS2, respectively (Table 2). With respect to the entire salt budget, for which the diffusive salt flux divergences are comparable in magnitude to the advective salt flux divergences, either the total mean or the total tidal pumping amounts to roughly 25% of the total salt balance, and this may vary somewhat from section to section.

5. The three dimensional nature of the salt fluxes

Thus far we considered the experiment duration (91 days) average salt balance, i.e., the divergence of salt flux by the three-dimensional circulation, plus the divergence of the turbulent diffusive salt flux both horizontally and vertically. A much simpler matter is the salt flux itself, free from the complexities introduced by spatial gradients. Shown in Fig. 13 for the Middle Tampa Bay section CS2 are the distributions in cross section view of the section normal (upper panels), section transverse (middle panels) and

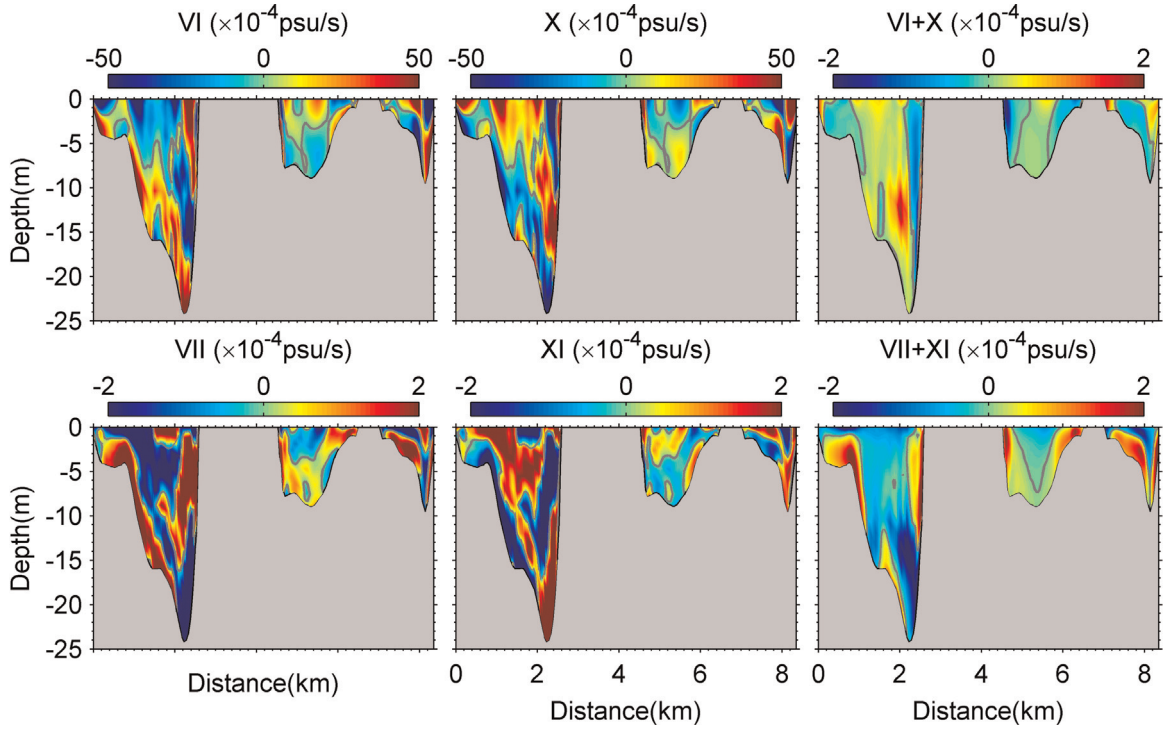

Fig. 11. The structures of the advective salt flux divergence terms after decomposition into mean and tidal pumping contributions evaluated at the Tampa Bay Mouth cross section CS1. The top panels show the horizontal and vertical mean flow terms (VI) and (X), respectively, and their sum (VI+X), and the bottom panels show the horizontal and vertical tidal pumping terms (VII) and (XI), respectively and their sum (VII+XI). Note that the mean flow terms (VI) and (X) are an order of magnitude larger than the tidal pumping terms (VII) and (XI), as indicated by the different colorbar scales. (For interpretation of the references to color in this figure legend, the reader is referred to the web version of this article.)

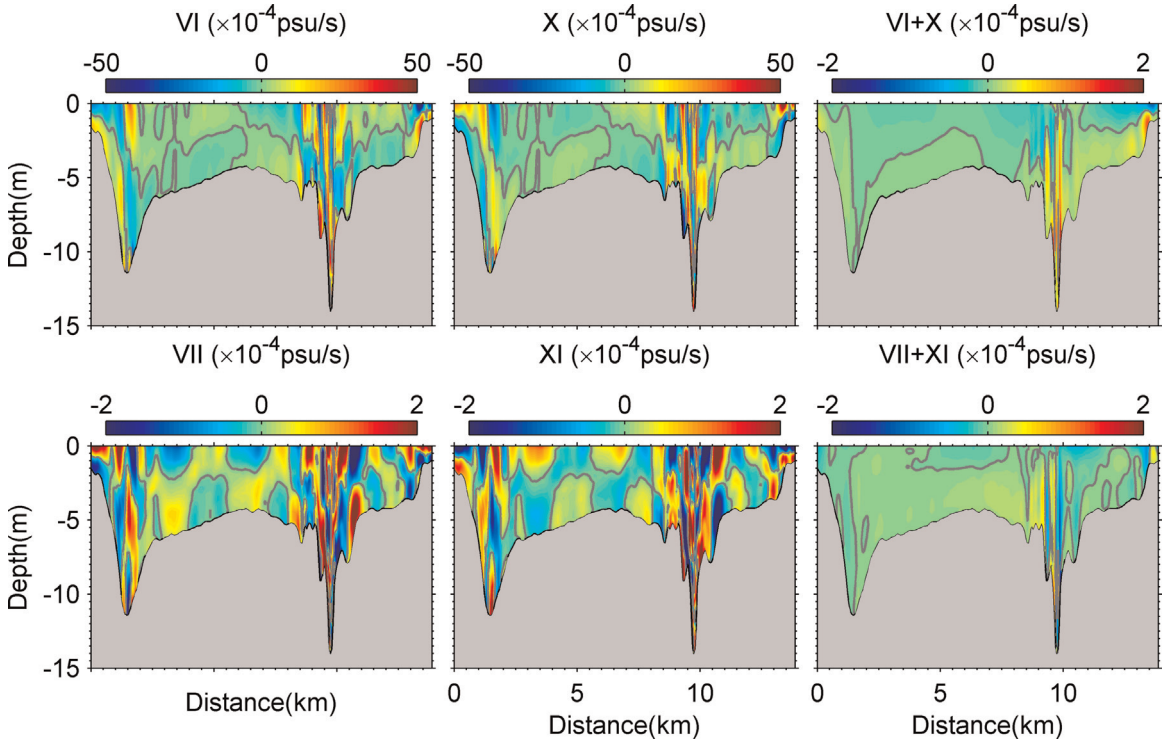

Fig. 12. Same as Fig. 11, except evaluated at the Middle Tampa Bay cross section CS2. (For interpretation of the references to color in this figure legend, the reader is referred to the web version of this article.)

the vertical constituents of the experiment duration average total salt flux. These are further decomposed (from left to right) into products of mean values, correlations between the fluctuating values (tidal pumping) and their sum, an example of which for the section normal component is given by Eq. (10):

$$\underset{\text{XII}}{\langle u_n S\rangle} = \underset{\text{XIII}}{\langle u_n\rangle\langle S\rangle} + \underset{\text{XIV}}{\langle u_n' S'\rangle} \tag{10}$$

where u_n the velocity component normal to the cross section and the right hand terms (XIII) and (XIV) are the contributions by the mean quantities and the tidal pumping, respectively.

For CS2, the normal component of the salt flux is primarily attributed (by an order of magnitude) to the product of the mean values (XIII) such that the sum of the mean and tidal pumping contributions (XIII+XIV) looks very similar to the mean contribution (XIII). The same can be said of the transverse and vertical components. In other words, the salt flux is primarily due to the mean circulation, versus the tidal pumping. Next we see that the transverse component (i.e. the across axis component) exhibits convergences and divergences, particularly about the locations of the shipping channels. This explains the cellular nature of the flux divergences shown in Section 4 and also the complex distribution of vertical salt flux in Fig. 13 that arises through such secondary circulations.

Owing to the Tampa Bay along axis variations in cross section and the relative positions of the various shipping channels, the along axis salt flux also varies with location. Fig. 14 addresses this for the Tampa Bay Mouth (CS1), Middle Tampa Bay (CS2), and Hillsborough Bay Mouth (CS3) cross sections. The flux by tidal pumping relative to the flux by the mean quantities is small at all of these. CS1 has the most complex structure by virtue of multiple ingress/egress and deepest depths. Particularly important is the central portion of Egmont Channel for the main ingress of salt to Tampa Bay. Next in complexity is CS2, where the existence of two shipping channels results in a net inflow within these channels and their vicinity, versus a net outflow over the shallower region in between them. The simplest distribution, and the one most aligned with the classical concept of a partially mixed estuary, is CS3, where occurs only one channel. There we see inflow in the lower portion and outflow in the upper portion of the water column, respectively, over the entire cross section, i.e., the classical two layer estuary circulation.

6. Summary and conclusions

A three-dimensional, high resolution numerical circulation model is used to diagnose the salt balance of Tampa Bay, a partial to well mixed estuary located on Florida's west coast. The model is an adaptation of the unstructured grid, Finite Volume Coastal Ocean Model (FVCOM) of Chen et al. (2003) that was applied to Tampa Bay at lower resolution by Weisberg and Zheng (2006). Using the same forcing conditions, Zhu et al. (2014a, 2014b) respectively explored the effects on model performance of increasing horizontal resolution to better resolve the shipping channels and other important conveyances of mass and how increased resolution bears upon the flushing of Tampa Bay as a whole and for selected sub-regions. Given the fidelity shown between the model simulation and the available observations, the present paper provides a detailed accounting of the salt balance and salt flux distributions for Tampa Bay using the same 91 day simulation interval: September to December, 2001.

The diagnoses are based on a model run forced by tides and rivers only so that we could concentrate on fluxes driven by gravitational convection and tidal pumping, unencumbered by wind effects. Salt balances are provided at the surface and near the bottom and for cross sections of varying complexity from the bay mouth, with its multiple openings, to the mouth of Hillsborough Bay with a simpler topography and a single shipping channel. For each of these planar or cross sections we calculate the terms comprising the conservation of salt, i.e., the advective salt flux divergences in the horizontal and vertical directions, the turbulent

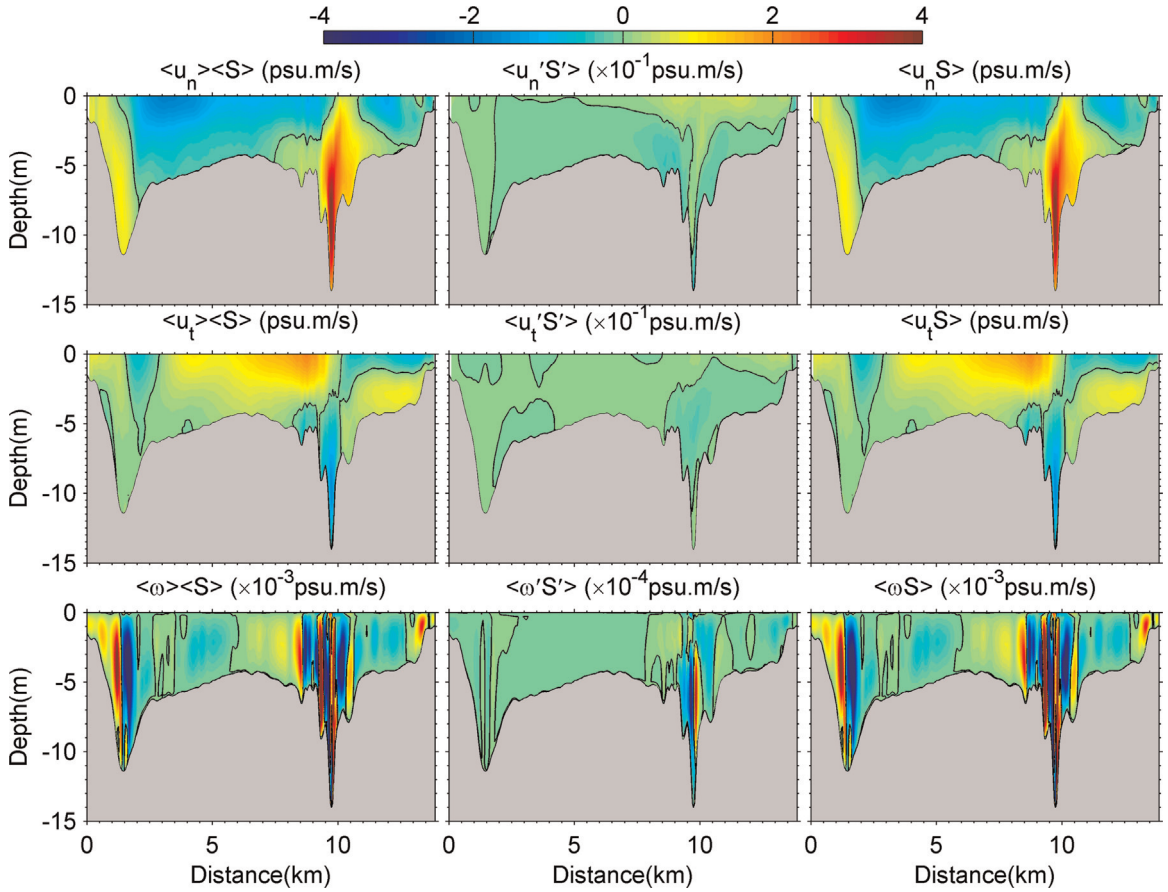

Fig. 13. The section normal (upper panels), section transverse (middle panels) and vertical (lower panels) components of the experimental duration average salt flux decomposed into the product of the mean values (left panels), tidal pumping (middle panels) and their sum (right panels) evaluated at the Middle Tampa Bay cross section CS2. The color bar sign convention is such that positive (negative) normal, transverse and vertical fluxes per unit area are directed into (out of) the page, to the right (left) and up (down), respectively. While the colorbar scale is the same, note the magnitude differences as indicated for each of the panels. In particular, the tidal pumping terms are an order of magnitude smaller than the corresponding mean terms. (For interpretation of the references to color in this figure legend, the reader is referred to the web version of this article.)

diffusive salt flux divergences in the horizontal and vertical directions and the local rate of change of salt. To examine the role of tidal pumping, or the correlation between the fluctuations in salinity and velocity, we further decompose the experimental mean advective salt flux divergences into divergences of the experimental duration mean salinity and velocity products and the tidal pumping. The primary findings associated with salt budgets in this paper are summarized in Fig. 15.

The premise of Fig. 15 is that the balances, regardless of location, are fully three-dimensional. Thus the upper left hand boxes consider the horizontal and vertical advective salt flux divergences, terms II and III, respectively, in Eq. (1) to consist of mean quantities (terms VI and X in the horizontal and vertical, respectively) and tidal pumping (terms VII and XI in the horizontal and vertical, respectively). Upon summation, the advective salt flux divergences in the horizontal and vertical directions tend to be counterbalancing, either for the mean quantities or the tidal pumping. For the mean quantities, the sum is a small residual of the much larger horizontal and vertical components, whereas for the tidal pumping, the sum, while smaller than the counterbalancing components, retains the same order of magnitude as the components. Further summation of the total (horizontal plus vertical) mean quantities (VI+X) with the total tidal pumping (VII+XI) constitutes the total advective salt flux divergence (II+III). The total advective salt flux divergence is then balanced primarily by the vertical diffusive salt flux divergence (V) except near the bottom of the shipping channels where the horizontal diffusive salt flux divergence (IV) also comes into play (because of the large derivatives and curvatures there). The pairs of numbers provided in Fig. 15 are the relative contributions [Eq. (8)] that these various terms make in summing to the experimental duration local rate of change of salinity at the surface (numbers on the left) and near bottom (numbers on the right). Taking some license in rounding the numbers, we summarize by saying: the overall balance is roughly half advection and half diffusion and the advection is roughly half mean quantity and half tidal pumping, where the finer details depend upon location (surface or bottom, shipping channel or shoals). An inescapable conclusion, regardless of the details, is that the salt balance is fully three-dimensional, and hence neglect of any of the coordinate directions would lead to spurious results.

A diagnosis of the salt flux components leads to a similar conclusion. Here we see (in Fig. 13) important contributions in all three coordinate directions, consistent with secondary circulations, a result being the cellular nature of the flux divergences. In going from the most complex (the Tampa Bay mouth with multiple ingress/egress and deepest depths) to the simplest (the Hillsborough Bay mouth with one channel) of the cross sections we see different across section distributions of the net influxes and effluxes of salt. Egmont Channel is the main conveyance of salt into Tampa Bay by virtue of depth. At mid-bay, with two channels, one on either side and with a shoal area in between, the influx of salt occurs across the entire water column in the main shipping channel, whereas the efflux of salt occurs in the shoal area in

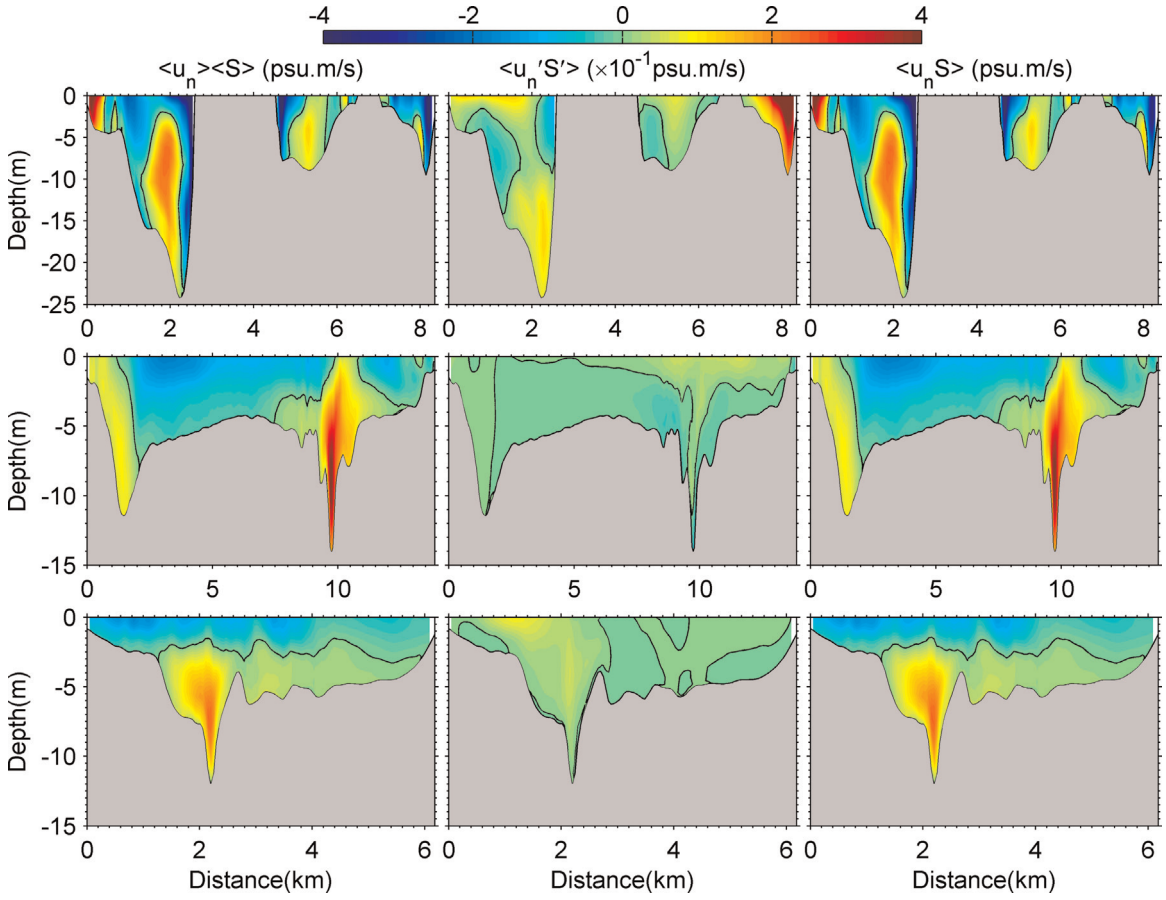

Fig. 14. The section normal experimental duration average salt flux by the product of the mean values (left panels), tidal pumping (middle panels) and their sum (right panels) evaluated at the Tampa Bay mouth cross section CS1 (upper panels), the Middle Tampa Bay cross section CS2 (middle panels) and the Hillsborough Bay mouth cross section CS3 (lower panels). The color bar sign convention is such that positive (negative) normal fluxes per unit area are directed into (out of) the page. While the colorbar scale is the same, note the magnitude differences as indicated for each of the panels. In particular, the tidal pumping terms are an order of magnitude smaller than the corresponding mean terms. (For interpretation of the references to color in this figure legend, the reader is referred to the web version of this article.)

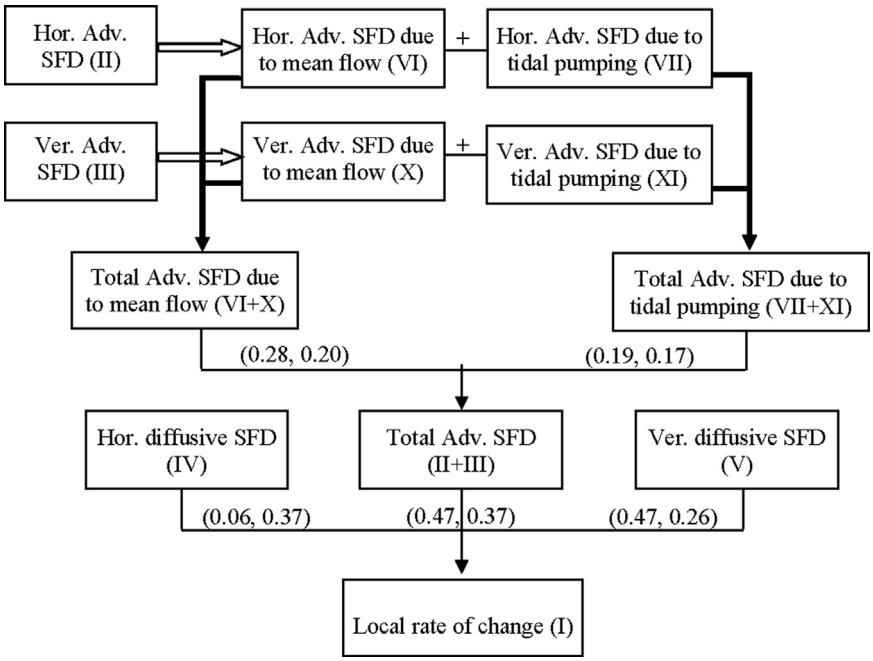

Fig. 15. A logical chart of the salt balance. Hor., Ver., Adv. and SFD are abbreviations for horizontal, vertical, advection and salt flux divergence, respectively. The pairs of numbers in brackets are the relative contribution ratios of the corresponding term to the experimental duration total rate of salinity change at the surface (left number) and near the bottom (right number). We note that terms II, III, VI and X are order 10^{-3}, whereas the other terms are order 10^{-4} (except for the very small local rate of change term I).

between. At the Hillsborough Bay mouth a much more classical two-layer estuary circulation is seen, but with the bulk of the influx associated within the shipping channel. Thus the structure of the circulation and the conveyances of mass may vary throughout an estuary depending upon geometry and fresh water source distributions. Regardless of the varying structures throughout Tampa Bay, the fluxes are dominated by the mean quantities, versus the tidal pumping, which are an order of magnitude smaller than the mean quantities. This is consistent with simpler model geometries such as MacCready (1999) in which the exchange flow (the mean baroclinic estuary circulation) is found to dominate the up estuary salt flux.

In general, despite very complex spatial structures evident in the horizontal and vertical advective flux divergences (overall means or Reynolds' decompositions), when summed three-dimensionally the patterns are relatively simple. Advection is balanced by diffusion (almost entirely by vertical diffusion except near the bottom of the deep shipping channel where horizontal gradients are large). The tendencies between these two effects (advection/diffusion) are such that near the surface advection tends to decrease whereas diffusion tends increase salinity, and conversely near the bottom, where advection tends to increase whereas diffusion tends to decrease salinity. This, of course, is not a new concept, as it was introduced observationally by Pritchard (1954) six decades ago before the advent of numerical techniques. The details, however, require such techniques.

For the instantaneous balances, versus the experimental duration means, the local rate of change of salinity is primarily due to the advective salt flux divergence with the diffusive salt flux divergences of lesser importance, the vertical portion everywhere and the horizontal portion only near the deep shipping channel bottom. The transition from the instantaneous to the mean balances occurs once the tides are filtered out from the analyses.

In conclusion:

(1) The salt balance for Tampa Bay is fully three dimensional.
(2) The horizontal and vertical advective salt flux divergences associated with mean quantities are equally large and tend to counterbalance, with their sum being a small, but significant residual.
(3) The horizontal and vertical advective salt flux divergences associated with tidal pumping are relatively small and counterbalancing, but when summed their residual is comparable in magnitude to that by the mean quantities.
(4) Adding the total advective salt flux divergence by the mean quantities and tidal pumping results in a tendency that is balanced primarily by vertical diffusion, except near the bottom of the deep channels where horizontal diffusion is also important.
(5) For the present study, without consideration of wind effects, the local instantaneous rate of salinity change is primarily controlled by the advective salt flux divergence, with secondary contributions by the vertical diffusive salt flux divergence everywhere and the horizontal diffusive salt flux divergence near the channel bottom.
(6) The salt fluxes (per unit area) themselves are fully three dimensional, exhibiting the effects of secondary circulations. The salt fluxes vary along the estuary axis with varying geometry and channel complexity; but, regardless of these variations, the salt fluxes by the mean quantities are much larger than the salt fluxes by tidal pumping.

With Tampa Bay being typical of many coastal plain estuaries with respect to geometrical complexity and tidal range, these findings likely find counterparts elsewhere. Finally, what we find for salt flux has implications for other state variables of ecological importance such as nutrients, fish larvae, algae, etc. How passive quantities, subjected to circulation, become distributed throughout the estuary will follow similar principles.

Acknowledgments

This work derives from a portion of J. Zhu's Ph.D. dissertation. Dr. Zhu was supported by a China Scholarship Council Award that facilitated his residence at the University of South Florida while a student at Ocean University of China, Qingdao, China. This work benefited from the National Science Foundation, Extreme Science and Engineering Discovery Environment (XSEDE) Program, Award #OCE130015 through which we were able to conduct the necessary model runs. Application support was also provided by the National Natural Science Foundation of China award #41106076 and Scientific Research Foundation of Third Institute of Oceanography, SOA award #2014025. We thank C. Chen (University of Massachusetts, Dartmouth) for graciously sharing the FVCOM code. J. Donovan assisted with computational matters at USF. Helpful comments and suggestions were provided by four anonymous reviewers.

References

Becker, M., Luettich, R., Seim, H., 2009. Effects of intratidal and tidal range variability on circulation and salinity structure in the Cape Fear River Estuary, North Carolina. J. Geophys. Res. 114 (C4), C04006. http://dx.doi.org/10.1029/2008JC004972.

Bowden, K., Sharaf El Din, S., 1966a. Circulation, salinity and river discharge in the Mersey Estuary. Geophys. J. R. Astron. Soc. 10, 383–399.

Bowden, K., Sharaf El Din, S., 1966b. Circulation and mixing processes in the Liverpool Bay area of the Irish Sea. Geophys. J. R. Astron. Soc. 11, 279–292.

Bowen, M., Geyer, W.R., 2003. Salt transport and the time-dependent salt balance of a partially stratified estuary. J. Geophys. Res. 108 (C5), 3185. http://dx.doi.org/10.1029/2001JC001231.

Burwell, D., Vincent, M., Luther, M., Galperin, B., 2000. Modeling residence times: Eulerian vs Lagrangian. In: Spaulding, M.L., Butler, H.L. (Eds.), Estuarine and Coastal Modeling. American Society of Civil Engineers, Reston, VA, pp. 995–1009.

Chant, R.J., 2002. Secondary flows in a region of flow curvature: relationship with tidal forcing and river discharge. J. Geophys. Res. 107, 3131 10.1023/2001JC001082.

Chen, C., Beardsley, R., Franks, P., 2001. A 3-D prognostic numerical model study of the Georges Bank ecosystem. Part I: physical model. Deep Sea Res. Part II: Top. Stud. Oceanogr. 48, 419–456.

Chen, C., Liu, H., Beardsley, R., 2003. An unstructured, finite-volume, three-dimensional, primitive equation ocean model: application to coastal ocean and estuaries. J. Atmos. Ocean. Technol. 20, 159–186.

Chen, S., Sanford, L., 2009. Axial wind effects on stratification and longitudinal salt transport in an idealized, partially mixed estuary. J. Phys. Oceanogr. 39 (8), 1905–1920. http://dx.doi.org/10.1175/2009JPO4016.1.

Dyer, K., 1974. The salt balance in stratified estuaries. Estuar. Coast. Mar. Sci. 2, 275–281.

Dyer, K., Gong, W., Ong, J., 1992. The cross sectional salt balance in a tropical estuary during a lunar tide and a discharge event. Estuar. Coast. Shelf Sci. 34, 579–591.

Egbert, G.D., Erofeeva, S.Y., 2002. Efficient inverse modeling of barotropic ocean tides. J. Atmos. Ocean. Technol. 19, 183–204.

Fischer, H., 1976. Mixing and dispersion in estuaries. Ann. Rev. Fluid Mech. 8, 107–133.

Fram, J., Martin, M., Stacey, M., 2007. Dispersive fluxes between the coastal ocean and a semienclosed estuarine basin. J. Phys. Oceanogr. 37 (6), 1645–1660. http://dx.doi.org/10.1175/JPO3078.1.

Galperin, B., Blumberg, A., Weisberg, R.H., 1991a. A time-dependent three-dimensional model of circulation in Tampa Bay. In: Treat, S., Clark, P. (Eds.), Proceedings of the Tampa Bay Area Scientific Information Symposium, vol. 2, Tampa, FL, pp. 77–97.

Galperin, B., Blumberg, A., Weisberg, R.H., 1991b. The importance of density driven circulation in well mixed estuaries: The Tampa Bay experience. In: Spaulding, M.L., Blumberg, A. (Eds.), Estuarine and Coastal Modeling. American Society of Civil Engineers, Tampa, FL, pp. 332–343.

Geyer, W.R., Nepf, H.M., 1996. Tidal pumping of salt in a moderately stratified estuary. In: Aubrey, D.G., Friedrichs, C.T. (Eds.), Buoyance Effects on Coastal and Estuarine Dynamics, Coastal and Estuarine Studies vol. 53. AGU, Washington, D. C, pp. 213–226.

Gong, W., Shen, J., 2011. The response of salt intrusion to changes in river discharge and tidal mixing during the dry season in the Modaomen Estuary China. Cont. Shelf Res. 31 (7), 769–788. http://dx.doi.org/10.1016/j.csr.2011.01.011.

Hansen, D., Rattray, M., 1965 Currents and mixing in the Columbia River estuary. In: Ocean Science and Ocean Engineering, vol. 2. The Marine Technology Society, Washington, DC, pp. 943–955.
He, R., Weisberg, R.H., 2002. West Florida shelf circulation and temperature budget for the 1999 spring transition. Cont. Shelf Res. 22 (5), 719–748.
He, R., Weisberg, R.H., 2003. West Florida shelf circulation and temperature budget for the 1998 fall transition. Cont. Shelf Res. 23, 777–800. http://dx.doi.org/10.1016/S0278-4343(03)00028-1.
Hughes, F., Rattray, M., 1980. Salt flux and mixing in the Columbia River estuary. Estuar. Coast. Mar. Sci. 10, 479–493.
Jia, P., Li, M., 2012. Circulation dynamics and salt balance in a lagoonal estuary. J. Geophys. Res. 117, C01003. http://dx.doi.org/10.1029/2011JC007124.
Kantha, L.H., Clayson, C.A., 2000. Numerical Models of Oceans and Oceanic Processes. Academic Press, San Diego, CA, p. 940.
Lewis, R., Estevez, E., 1988. Ecology of Tampa Bay, Florida: An Estuarine Profile. US Department of the Interior, National Wetlands Research Center, Washington, DC.
Lerczak, J.A., Geyer, W.R., 2004. Modeling the lateral circulation in straight, stratified estuaries. J. Phys. Oceanogr. 34, 1410–1428.
Lerczak, J., Geyer, W.R., Chant, R., 2006. Mechanisms driving the time-dependent salt flux in a partially stratified estuary. J. Phys. Oceanogr. 36 (12), 2296–2311.
MacCready, P., 1999. Estuarine adjustment to changes in river flow and tidal mixing. J. Phys. Oceanogr. 29 (4), 708–726.
MacCready, P., Geyer, W.R., 2010. Advances in estuarine physics. Ann. Rev. Mar. Sci. 2, 35–58.
Mellor, G.L., Yamada, T., 1982. Development of a turbulence closure model for geophysical fluid problems. Rev. Geophys. 20, 851–875.
Meyers, S., Luther, M., 2008. A numerical simulation of residual circulation in Tampa Bay. Part II: Lagrangian residence time. Estuar. Coasts 31 (5), 815–827. http://dx.doi.org/10.1007/s12237-008-9085-0.
Meyers, S., Luther, M., Wilson, M., Havens, H., Linville, A., Sopkin, K., 2007. A numerical simulation of residual circulation in Tampa Bay. Part I: low-frequency temporal variations. Estuar. Coasts 30 (4), 679–697.
Nepf, H., Geyer, W.R., 1996. Intratidal variations in stratification and mixing in the Hudson estuary. J. Geophys. Res. **101** (C5), 12079–12086.
Nunes, R.A., Simpson, J.H., 1985. Axial convergence in a well mixed estuary. Estuar. Coast. Mar. Sci. 20, 637–649.
Pritchard, D., 1954. A study of the salt balance in a coastal plain estuary. J. Mar. Res. 13 (1), 133–144.
Ralston, D., Geyer, W.R., Lerczak, J., 2010. Structure, variability, and salt flux in a strongly forced salt wedge estuary. J. Geophys. Res. 115, C06005. http://dx.doi.org/10.1029/2009JC005806.
Rattray, M., Dworski, J., 1980. Comparison of methods for analysis of the transverse and vertical circulation contributions to the longitudinal advective salt flux in estuaries. Estuar. Coast. Mar. Sci. 11, 515–536.
Simpson, J., Vennell, R., Souza, A., 2001. The salt fluxes in a tidally-energetic estuary. Estuar. Coast. Shelf Sci. 52, 131–142.
Smagorinsky, J., 1963. General circulation experiments with the primitive equations: I. The basic experiment. Mon. Weather Rev. 91, 99–164.
Soltaniasl, M., Kawanisi, K., Yano, J., Ishikawa, K., 2013. Variability in salt flux and water circulation in Ota River Estuary, Japan. Water Sci. Eng. 6 (3), 283–295.
Uncles, R., Jordan, M., 1979. Residual fluxes of water and salt at two stations in the Severn Estuary. Estuar. Coast. Mar. Sci. 9, 287–302.
Vincent, M., Burwell, D., Luther, M., 2000. The Tampa Bay nowcast–forecast system. In: Spaulding, M.L., Butler, H.L. (Eds.), Estuarine and Coastal Modeling, pp. 765–780.
Weisberg, R.H., Williams, R., 1991. Initial findings on the circulation of Tampa Bay. In: Treat, S., Clark, P. (Eds.), Proceedings of Tampa Bay Area Scientific Information Symposium, vol. 2, Tampa, FL, pp. 49–66.
Weisberg, R.H., Zheng, L.Y., 2003. How estuaries work: a Charlotte Harbor example. J. Mar. Res. 61, 635–657.
Weisberg, R.H., Zheng, L.Y., 2006. Circulation of Tampa Bay driven by buoyancy, tides, and winds, as simulated using a finite volume coastal ocean model. J. Geophys. Res. 111, C01005. http://dx.doi.org/10.1029/2005JC003067.
Weisberg, R.H., 2011. Coastal ocean pollution, water quality and ecology. Mar. Technol. Soc. J. 45, 35–42.
Whitney, M.M., Allen, J.S., 2008. Coastal wind-driven circulation in the vicinity of a bank. Part I: modeling flow over idealized symmetric banks. J. Phys. Oceanogr. 39, 1273–1297.
Wu, H., Zhu, J., Choi, B., 2010. Links between saltwater intrusion and subtidal circulation in the Changjiang Estuary: a model-guided study. Cont. Shelf Res. 30, 1891–1905. http://dx.doi.org/10.1016/j.csr.2010.09.001.
Zhang, A., Wei, E., 2010. Development of NOAA's Tampa Bay operational forecast system. In: Spaulding, M.L. (Ed.), Estuarine and Coastal Modeling. American Society of Civil Engineers, Reston, VA, pp. 686–703.
Zheng, L.Y., Weisberg, R.H., 2012. Modeling the west Florida coastal ocean by downscaling from the deep ocean, across the continental shelf and into estuaries. Ocean Model. 48, 10–29.
Zhu, J., Weisberg, R.H., Zheng, L.Y., Han, S., 2014a. Influences of channel deepening and widening on the tidal and non-tidal circulation of Tampa Bay. Estuar. Coasts 38, 132–150. http://dx.doi.org/10.1007/s12237-014-9815-4.
Zhu, J., Weisberg, R.H., Zheng, L.Y., Han, S., 2014b. On the flushing of Tampa Bay. Estuar. Coasts 38, 118–131. http://dx.doi.org/10.1007/s12237-014-9793-6.